# On the Crossed Field Antenna Performance

Valentino Trainotti, *Senior Member, IEEE,* and Luis A. Dorado, *Student Member, IEEE*

***Abstract*— Lately, short antennas and Crossed Field Antennas (CFA) have attracted broadcast and amateur community attention.**

**The CFA antenna has been developed in the last decade of the 20th century, trying to obtain a compact transmitting antenna for low and medium frequency AM bands. The CFA is intended to be used in order to get a low profile antenna and a supposed performance similar or better compared to a quarter-wave monopole.**

**The CFA has a short monopole and a metallic disk close to the monopole base, both mechanical structures being fed by means of two separated generators. Thus, the CFA has two ports and can be analyzed from the Network Theory point of view.**

**In this paper, the CFA has been studied exhaustively using the Transmission Line Method (TLM) in order to obtain an equivalent network and the antenna performance. Due to the lack of theoretical data to explain the CFA antenna behavior, the TLM has been validated by means of Moment Method simulations and some available experimental data.**

**As a first approximation, the CFA is placed on a perfectly electric conducting (PEC) ground plane in order to obtain the antenna currents and near fields. Once this task has been performed, losses due to an actual ground and an artificial metallic ground plane, that is of common use in practice, can be calculated.**

**The novel approach here permits to obtain the near and far field expressions from the current distributions on the antenna structure. Then, near field calculations are used to determine the surface current density on the ground plane around the antenna and the wave impedance as a function of distance in space.**

**Near fields and wave impedance are used for determining whether the Poynting Vector Synthesis (PVS) phenomenon exists or not. PVS means that the far field zone boundary is located at the surface of the CFA antenna structure itself, the power density or Poynting vector being real everywhere in space.**

**From the artificial and natural ground plane surface current density, the power dissipation is calculated in a circular boundary half-wavelength from the antenna base, and the ground plane equivalent loss resistance is obtained.**

**Artificial ground plane behavior is paramount in obtaining the best performance of a CFA antenna due to its short height in wavelengths, as well as in any monopole antenna type.**

***Index Terms*— CFA, Crossed Field Antenna, CFA Antenna, LF Antennas, LF Broadcast Antennas, LF Broadcast Transmitting Antennas, LF AM Broadcast Antennas, LF Monopole Antennas, MF Antennas, MF Broadcast Antennas, MF Broadcast Transmitting Antennas, LF Short Transmitting Antennas, MF Short Transmitting Antennas, MF AM Broadcast Antennas, MF Monopole Antennas, Short monopole, Top-loaded monopole, Ground plane, Grounding, Antenna Input Impedance, Antenna Efficiency, Antenna Gain, Antenna Performance, Antenna Bandwidth.**

V. Trainotti is with University of Buenos Aires, Argentina (e-mail: vtrainotti@ieee.org).
L. A. Dorado is with University of Buenos Aires, Argentina (e-mail: luis_dorado@ieee.org).

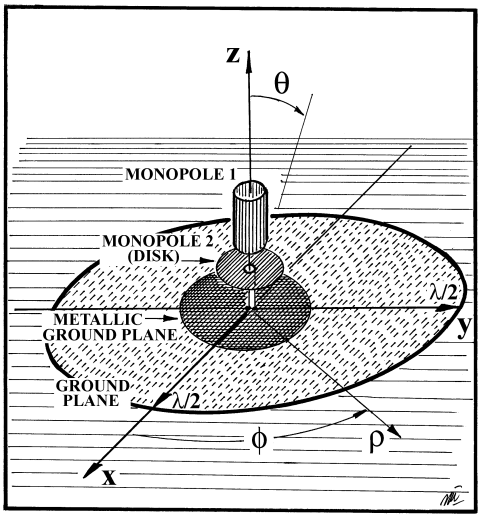


Fig. 1. Crossed Field Antenna (CFA) general sketch.

## I. Introduction

ANY linear antenna is a Crossed Field Antenna (CFA) in the far field zone, in the sense that the electric field is perpendicular to the magnetic field in space and both fields are perpendicular to the direction of wave propagation, which is indicated by a real power density or Poynting vector.

Nevertheless, the term CFA was intended to be used for an antenna where the existence of the crossed fields is everywhere in space, which is known as Poynting Vector Synthesis (PVS). Calculations demonstrate that this is a utopia, because on the antenna metallic structure both fields must fulfill the boundary conditions and a near field zone always exists, where induction fields predominate.

The CFA antenna has a short monopole (monopole 1) and another very short monopole (monopole 2) with a metallic disk as a top-load, which is parallel and close to the earth. The dimensions of both metallic structures, monopoles 1 and 2, are much smaller than the wavelength, then the Transmission Line Method (TLM) for the analysis of top-loaded monopoles applies [1]. The monopole 1 axis passes through a hole at the disk center, as can be seen in Fig. 1.

Generally, the ground below the antenna structure is covered by a thin metallic layer whose diameter is greater than the metallic disk.

Input power is injected into the antenna by means of two generators, the first one is connected to the monopole 1 base and ground and the second one is connected to the monopole 2 (disk) and ground.

In this paper, the CFA antenna was thoroughly analyzed from the input impedance and radiation properties points of view using Maxwell equations through the TLM and a

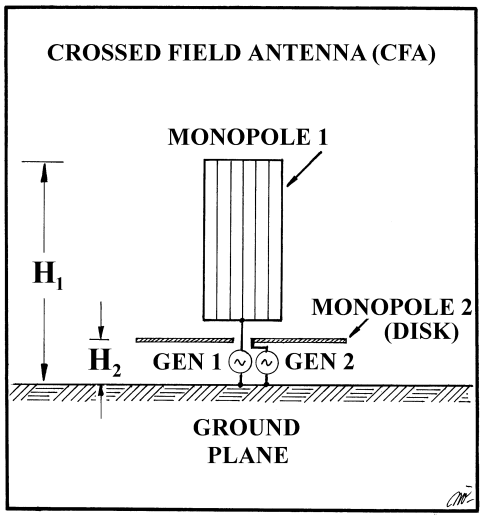


Fig. 2. Crossed Field Antenna (CFA) feeding system.

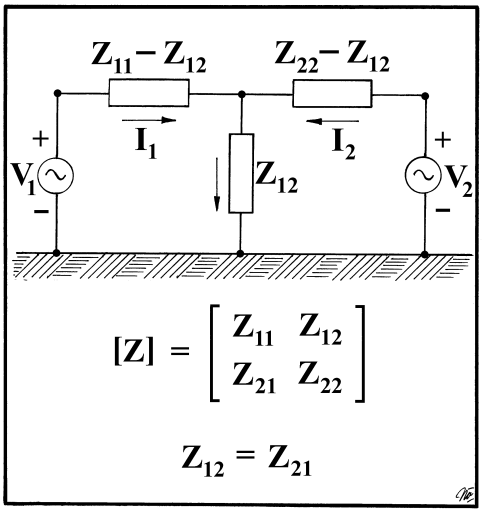


Fig. 3. Crossed Field Antenna (CFA) equivalent network.

Moment Method approach. No serious theoretical analysis of this antenna has been found in the technical literature and only partial analysis made up by software simulations [2]–[5] or some experiment with actual and reduced scale models [6]–[10]. Both intents do not explain clearly the actual antenna performance, inventors explanations are too vague and they do not support their invention by means of a clear theory in order to assure its working performance [11]–[16].

## II. Equivalent Network

The CFA antenna can be analyzed from a network point of view, taking into account the two ports in the antenna structure. Monopole 1 base and ground are the port 1 terminals, while metallic disk (monopole 2) and ground are the port 2 terminals. A sketch of this antenna can be seen in Fig. 2.

Generators are connected to both monopoles, 1 and 2 (disk), with short leads as it is usual in high and very high frequency techniques. Pictures of some published CFA antennas have their feeding connections with long wires placed in the space occupied by the near fields. It seems that this technique is the same as used by electrical 50 or 60 Hz installations and it should be avoided in RF frequency systems.

The antenna equivalent network can be characterized by its impedance parameters, the monopole 1 self-impedance, $\mathrm{Z}_{11}$, the monopole 2 self-impedance (disk), $\mathrm{Z}_{22}$, and the mutual impedances, $\mathrm{Z}_{12}$ and $\mathrm{Z}_{21}$, between them.

Fig. 3 shows the antenna equivalent network, where a generator is connected to each port. Generator 1, connected to port 1, has a voltage $\mathrm{V}_1$, while generator 2, connected to port 2, has a voltage $\mathrm{V}_2$. As soon as both generators are connected to the antenna ports, currents $\mathrm{I}_1$ and $\mathrm{I}_2$ will flow into the antenna structure.

By using impedance parameters, the standard network equations can be written in matrix form as follows [17]–[19]:

$$\begin{bmatrix} \mathrm{V}_1 \\ \mathrm{V}_2 \end{bmatrix} = \begin{bmatrix} \mathrm{Z}_{11} & \mathrm{Z}_{12} \\ \mathrm{Z}_{21} & \mathrm{Z}_{22} \end{bmatrix} \cdot \begin{bmatrix} \mathrm{I}_1 \\ \mathrm{I}_2 \end{bmatrix} \tag{1}$$

From the Reciprocity Theorem, it follows that $\mathrm{Z}_{12} = \mathrm{Z}_{21}$.

Admittance parameters will also be required and are obtained by inverting the impedance matrix, that is

$$\mathrm{Y}_{11} = \mathrm{G}_{11} + \mathrm{j}\,\mathrm{B}_{11} = \frac{\mathrm{Z}_{22}}{\mathrm{Z}_{11}\,\mathrm{Z}_{22} - \mathrm{Z}_{12}^2} \tag{2}$$

$$\mathrm{Y}_{12} = \mathrm{Y}_{21} = \mathrm{G}_{12} + \mathrm{j}\,\mathrm{B}_{12} = -\frac{\mathrm{Z}_{12}}{\mathrm{Z}_{11}\,\mathrm{Z}_{22} - \mathrm{Z}_{12}^2} \tag{3}$$

$$\mathrm{Y}_{22} = \mathrm{G}_{22} + \mathrm{j}\,\mathrm{B}_{22} = \frac{\mathrm{Z}_{11}}{\mathrm{Z}_{11}\,\mathrm{Z}_{22} - \mathrm{Z}_{12}^2} \tag{4}$$

The impedance and admittance matrices are functions of frequency and the physical dimensions of the antenna system.

### A. Network Parameters

The CFA antenna can be considered as an array of two tightly coupled short monopoles. The first one is a monopole of height $\mathrm{H}_1$, which could have or not a top-load, while the second one is a monopole of height $\mathrm{H}_2$ with the disk as its top-load. These monopoles are shown in Figs. 4 and 5.

Thus, the present theory is based on the Transmission Line Method (TLM) outlined in [1] for the analysis of a top-loaded monopole [20].

When port 2 is an open circuit, the monopole 1 input impedance, $\mathrm{Z}_{11} = \mathrm{R}_{11} + \mathrm{j}\,\mathrm{X}_{11}$, is the impedance of a short monopole with a given degree of top-loading.

When port 1 is an open circuit, the monopole 2 input impedance, $\mathrm{Z}_{22} = \mathrm{R}_{22} + \mathrm{j}\,\mathrm{X}_{22}$, is the impedance of another very short monopole with the disk as its top-load (practically a Hertz monopole).

Self-resistance and reactance of each monopole are given by [1]

$$\mathrm{R}_{\mathrm{ii}} = \mathrm{R}_{\mathrm{radi}} + \mathrm{R}_{\mathrm{ci}} + \mathrm{R}_{\mathrm{gpi}} \qquad \mathrm{i} = 1,\ 2 \tag{5}$$

$$\mathrm{X}_{\mathrm{ii}} = \mathrm{Z}_{0\mathrm{mi}}\,\frac{\mathrm{Z}_{0\mathrm{mi}}\,\tan\beta\mathrm{H}_\mathrm{i} + \mathrm{X}_{\mathrm{ti}}}{\mathrm{Z}_{0\mathrm{mi}} - \mathrm{X}_{\mathrm{ti}}\,\tan\beta\mathrm{H}_\mathrm{i}} \qquad \mathrm{i} = 1,\ 2 \tag{6}$$

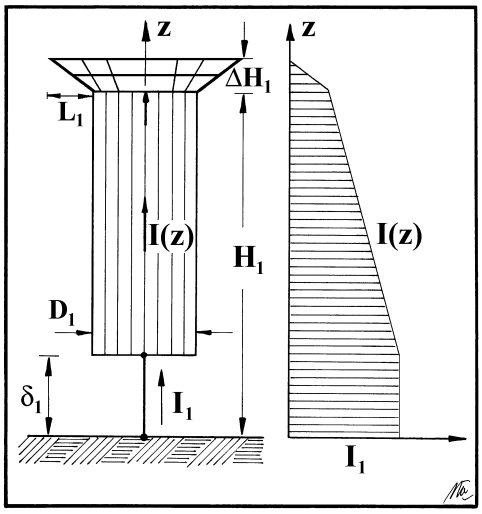


Fig. 4. CFA monopole 1 current distribution.

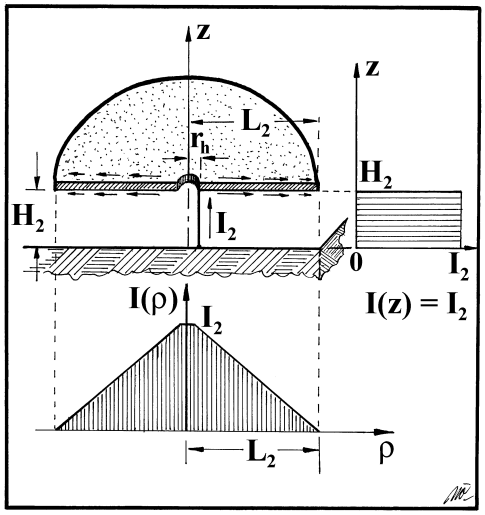


Fig. 5. CFA monopole 2 and top-loading disk current distributions.

Where

$R_{radi}$ is the i-th monopole radiation resistance [Ω].

$R_{ci}$ is the i-th monopole conductor resistance [Ω].

$R_{gpi}$ is the i-th monopole ground plane loss resistance [Ω].

$Z_{0mi}$ is the average characteristic impedance of the ith-monopole equivalent transmission line [1] [Ω].

$X_{ti}$ is the ith-monopole top-reactance [Ω].

$H_i$ is the ith-monopole height [m].

The i-th monopole radiation resistance is [21]–[23]

$$R_{radi} = 40\,(\beta H_{ei})^2 \qquad i = 1,\ 2 \tag{7}$$

Where $H_{ei}$ is the i-th monopole effective height, which depends on the vertical wire current distribution, and it is given by

$$\beta H_{ei} = \sin\beta H_i + \frac{X_{ii}}{Z_{0mi}}\,(1 - \cos\beta H_i) \qquad i = 1,\ 2 \tag{8}$$

Due to a very small disk height, $H_2$, over the ground plane and a disk radius, $L_2$, greater than this height, the current distribution on monopole 2 is practically constant, therefore

$$H_{e2} \cong H_2 \tag{9}$$

The top-reactance of monopole 1, $X_{t1}$, is [1]

$$X_{t1} = -\frac{Z_{0t1}}{n\,\tan\beta L_1} \tag{10}$$

Where

$Z_{0t1}$ is the monopole 1 top-load characteristic impedance [1] [Ω].

$L_1$ is the monopole 1 top-load length [m].

$n$ is the number of top-load branches of monopole 1.

The top-reactance of monopole 2, $X_{t2}$, is

$$X_{t2} = -\frac{1}{2\,\pi\,f\,C_2} \tag{11}$$

Where the disk capacitance, $C_2$, can practically be calculated as a simple capacitor with a circular plate of radius $L_2$ and a separation from the ground plane equal to the monopole 2 height, $H_2$, then

$$C_2 = \epsilon_0\,\frac{\pi\,L_2^2}{H_2} \tag{12}$$

When port 2 is an open circuit, the mutual impedance $Z_{21}$ is the ratio between the open circuit voltage in port 2 and the current flowing in port 1, that is

$$Z_{21} = \left.\frac{V_2}{I_1}\right|_{I_2 = 0} \tag{13}$$

Also, the open circuit voltage $V_2$ is due to the electric field $E_{z1}$ between the capacitor plate and ground [24], according to the current $I_1$ in port 1, then

$$Z_{21} = -\left.\frac{E_{z1}\,H_2}{I_1}\right|_{I_2 = 0} \tag{14}$$

The electric field $E_{z1}$ is the near field produced by monopole 1 in the space surrounding the antenna and can be calculated by means of (22).

Another possibility to calculate the impedance and admittance parameters is using the Method of Moments (MoM), which has been used extensively by means of our own software [25], but similar results could be obtained by means of other standard softwares. These parameters are practically the same for both techniques, Transmission Line Method (TLM) and MoM, as practical examples indicate.

Nevertheless, it is important to have at hands the electromagnetic equations in order to solve the problem and have a clear view of the antenna behavior.

### B. Input Impedances

The antenna is excited by means of two generators, for this reason, monopole 1 input voltage $\mathrm{V}_1$ will be taken as the phase reference and monopole 2 input voltage $\mathrm{V}_2$ will be given by

$$\mathrm{V}_2 \;=\; \mathrm{K}\,\mathrm{V}_1\,\mathrm{e}^{\mathrm{j}\,\phi_2} \tag{15}$$

Thus, the parameter K is the amplitude ratio between $\mathrm{V}_1$ and $\mathrm{V}_2$, while $\phi_2$ is the phase difference between them. Voltages and currents are taken as effective values.

The port 1 input impedance is

$$\mathrm{Z}_1 = \mathrm{R}_1 + \mathrm{j}\,\mathrm{X}_1 = \frac{\mathrm{V}_1}{\mathrm{I}_1} \;=\; \frac{1}{\mathrm{Y}_{11} + \mathrm{Y}_{12}\,\mathrm{K}\,\mathrm{e}^{\mathrm{j}\,\phi_2}} \tag{16}$$

The port 2 input impedance is

$$\mathrm{Z}_2 = \mathrm{R}_2 + \mathrm{j}\,\mathrm{X}_2 = \frac{\mathrm{V}_2}{\mathrm{I}_2} \;=\; \frac{\mathrm{K}}{\mathrm{Y}_{12}\,\mathrm{e}^{-\mathrm{j}\,\phi_2} + \mathrm{K}\,\mathrm{Y}_{22}} \tag{17}$$

It can be seen that the input impedances depend on a strong interaction between both generators.

### C. Input Power

The active or real power $\mathrm{W}_1 \;=\; |\mathrm{I}_1|^2\,\mathrm{R}_1$, produced by generator 1, is given by

$$\mathrm{W}_1 \;=\mid \mathrm{V}_1 \mid^2\; (\mathrm{G}_{11} + \mathrm{K}\,\mathrm{G}_{12}\,\cos\phi_2 - \mathrm{K}\,\mathrm{B}_{12}\,\sin\phi_2) \tag{18}$$

The active or real power $\mathrm{W}_2 \;=\; |\mathrm{I}_2|^2\,\mathrm{R}_2$, produced by generator 2, is given by

$$\mathrm{W}_2 \;=\mid \mathrm{V}_1 \mid^2\; (\mathrm{K}^2\,\mathrm{G}_{22} + \mathrm{K}\,\mathrm{G}_{12}\,\cos\phi_2 + \mathrm{K}\,\mathrm{B}_{12}\,\sin\phi_2) \tag{19}$$

Then, the total input power will be the sum of the input powers of both generators, $\mathrm{W}_{\mathrm{in}} = \mathrm{W}_1 + \mathrm{W}_2$, that is

$$\mathrm{W}_{\mathrm{in}} \;=\mid \mathrm{V}_1 \mid^2\; (\mathrm{G}_{11} + 2\,\mathrm{K}\,\mathrm{G}_{12}\,\cos\phi_2 + \mathrm{K}^2\,\mathrm{G}_{22}) \tag{20}$$

Equation (20) shows that the input power depends on the cosine of the voltage phase difference $\phi_2$. For this reason, there are three cases:

(I) When $\mathrm{G}_{12} > 0$, the input power is maximum for $\phi_2 = 0\ (360^\circ)$ and minimum for $\phi_2 = 180^\circ$.
(II) When $\mathrm{G}_{12} < 0$, the input power is maximum for $\phi_2 = 180^\circ$ and minimum for $\phi_2 = 0\ (360^\circ)$.
(III) When $\mathrm{G}_{12} = 0$, the input power is constant for any value of $\phi_2$.

These three cases or regimes depend on the antenna physical dimensions and frequency, and once these are given, the antenna will operate in only one of those regimes.

In Fig. 6, a CFA operating in the first regime is shown ($\mathrm{G}_{12} > 0$, $\phi_2 = 0$) as well as the antenna equivalent circuit, where the currents of both generators are in phase. In Fig. 7 a CFA operating in the second regime is shown ($\mathrm{G}_{12} < 0$, $\phi_2 = 180^\circ$), where the generator currents are out of phase. When $\mathrm{G}_{12} = 0$, the CFA will operate either as in Figs. 6 or 7 according to the highest voltage generator, however, the total input power will be independent of $\phi_2$.

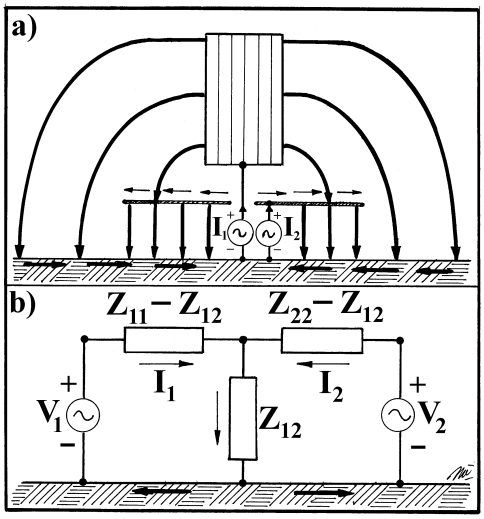


Fig. 6. a) CFA operating in the first regime (I) $\mathrm{G}_{12} > 0$. b) CFA equivalent circuit.

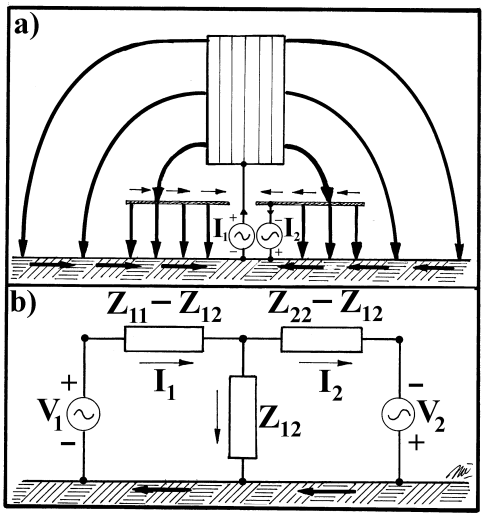


Fig. 7. a) CFA operating in the second regime (II) $\mathrm{G}_{12} < 0$. b) CFA equivalent circuit.

## III. Electromagnetic Field

The electromagnetic field radiated from the antenna is the sum of the radiation produced by the array of the two CFA monopoles. Monopole 1 is a top-loaded short vertical antenna and monopole 2 is practically a Hertz monopole makes up by the disk and its feeding vertical lead.

Because of the very short distance between both radiators, the radiation center is located on the CFA vertical geometric axis at a zero height. The feeding currents of each radiating source have different amplitudes and phases depending on the voltages of both generators.

### A. Near Field

The near field of a top-loaded monopole has been determined in [1] using Image Theory, according to Fig. 8 geometry.

Then, the magnetic and electric near fields of both monopoles on the ground plane, at $\mathrm{z} = 0$, are given by [1]

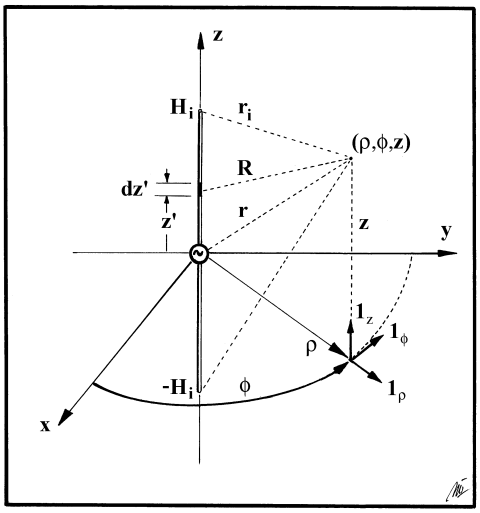


Fig. 8. Monopole geometry used to calculate the near field in cylindrical coordinates.

$$\mathrm{H}_{\phi \mathrm{i}} = -\frac{\mathrm{I}_{\mathrm{mi}}}{4\,\pi\,\rho}\left\{ \mathrm{e}^{\mathrm{j}\psi_{\mathrm{i}}}\left[\left(1-\frac{\mathrm{H_i}}{\mathrm{r_i}}\right)\mathrm{e}^{-\mathrm{j}\beta(\mathrm{r_i}+\mathrm{H_i})} - \mathrm{e}^{-\mathrm{j}\beta\rho}\right]\right. \quad (21)$$
$$\left. -\ \mathrm{e}^{-\mathrm{j}\psi_{\mathrm{i}}}\left[\left(1+\frac{\mathrm{H_i}}{\mathrm{r_i}}\right)\mathrm{e}^{-\mathrm{j}\beta(\mathrm{r_i}-\mathrm{H_i})} - \mathrm{e}^{-\mathrm{j}\beta\rho}\right]\right\}$$

$$\mathrm{E}_{\mathrm{zi}} = \frac{\mathrm{j}\,\mathrm{I}_{\mathrm{mi}}}{4\,\pi\,\epsilon_0\,\omega\,\rho} \quad (22)$$
$$\left\{ \mathrm{e}^{\mathrm{j}\psi_{\mathrm{i}}}\left[\frac{\rho\,\mathrm{e}^{-\mathrm{j}\beta(\mathrm{r_i}+\mathrm{H_i})}}{\mathrm{r_i}}\left(\frac{\mathrm{H_i}}{\mathrm{r_i^2}} - \mathrm{j}\,\beta\Big(1-\frac{\mathrm{H_i}}{\mathrm{r_i}}\Big)\right)\right.\right.$$
$$\left. + \mathrm{j}\,\beta\,\mathrm{e}^{-\mathrm{j}\beta\rho}\right] +$$
$$+\ \mathrm{e}^{-\mathrm{j}\psi_{\mathrm{i}}}\left[\frac{\rho\,\mathrm{e}^{-\mathrm{j}\beta(\mathrm{r_i}-\mathrm{H_i})}}{\mathrm{r_i}}\left(\frac{\mathrm{H_i}}{\mathrm{r_i^2}} + \mathrm{j}\,\beta\Big(1+\frac{\mathrm{H_i}}{\mathrm{r_i}}\Big)\right)\right.$$
$$\left.\left. -\ \mathrm{j}\,\beta\,\mathrm{e}^{-\mathrm{j}\beta\rho}\right]\right\}$$

Where $\mathrm{i} = 1,\ 2$ and

$$\mathrm{r_i} = \sqrt{\rho^2 + \mathrm{H_i^2}}$$

$$\mathrm{I_{mi}} = \mathrm{I_i}\sqrt{1+\left(\frac{\mathrm{X_{ii}}}{\mathrm{Z_{0mi}}}\right)^2}$$

$$\psi_{\mathrm{i}} = \arctan\left(\frac{\mathrm{X_{ii}}}{\mathrm{Z_{0mi}}}\right)$$

It is assumed, as in [1], that only the vertical part of a top-loaded monopole produces a net electromagnetic field. The distance $\rho$ along the surface of the earth is measured from the center of the cylindrical coordinates or antenna vertical axis.

The CFA total near electromagnetic fields on the ground plane ($\mathrm{z} = 0$) will be

$$\mathrm{H}_{\phi} = \mathrm{H}_{\phi 1} + \mathrm{H}_{\phi 2} \quad (23)$$

$$\mathrm{E_z} = \mathrm{E_{z1}} + \mathrm{E_{z2}} \quad (24)$$

On the surface of the earth, a thin metallic layer of radius $\mathrm{R}_0$ is laid down, which is called the *artificial ground plane*. From this metallic layer radius $\mathrm{R}_0$, the bare soil is considered up to a distance of half-wavelength. This is the surface of the earth to be taken into account in the soil power loss calculations.

Over the metallic layer or artificial ground plane the electric field is practically perpendicular, having only the $\mathrm{E_z}$ component, due to the boundary conditions of a very high conductivity medium, where the surface impedance $\mathrm{Z_g}$ is given by [26], [27]

$$\mathrm{Z_g} = \mathrm{R_g} + \mathrm{j}\,\mathrm{X_g} = \sqrt{\frac{\omega\,\mu_0}{2\,\sigma_{\mathrm{m}}}}\,(1+\mathrm{j}) \quad \text{for} \quad \rho < \mathrm{R}_0 \quad (25)$$

Where $\sigma_{\mathrm{m}}$ is the metallic layer conductivity.

On the bare soil, the electric field develops a radial component $\mathrm{E}_\rho$ due to the low conductivity compared to that of the metallic layer, and is given by

$$\mathrm{E}_\rho = -\mathrm{Z_s}\,\mathrm{H}_\phi \quad (26)$$

Where $\mathrm{Z_s}$ is the bare soil impedance, which can be calculated from the soil conductivity, $\sigma$, and permittivity, $\epsilon$, as follows [26], [27]

$$\mathrm{Z_s} = \mathrm{R_s} + \mathrm{j}\,\mathrm{X_s} = \sqrt{\frac{\mathrm{j}\,\omega\,\mu_0}{\sigma + \mathrm{j}\,\omega\,\epsilon}} \quad \text{for} \quad \rho > \mathrm{R}_0 \quad (27)$$

### *B. Wave Impedance*

The wave impedance in space, just above the earth surface in the air, is the ratio between the near electric and magnetic fields $\mathrm{E_z}$ and $\mathrm{H}_\phi$ on the ground plane, and is a function of distance $\rho/\lambda$, therefore

$$\mathrm{Z}_0 = -\frac{\mathrm{E_z}}{\mathrm{H}_\phi} \quad (28)$$

In the far field zone, $\rho \gg \lambda$, the wave impedance is practically equal to the free space intrinsic impedance $\mathrm{Z}_{00} = 120\pi\ \Omega$. The wave impedance $\mathrm{Z}_0$ is almost pure imaginary or reactive very close to the antenna and almost pure real or resistive at a distance greater than half-wavelength.

### *C. Far Field*

In the far field zone, when spherical coordinates are used, the CFA total far electric field $\mathrm{E}_\theta$ will be the sum of the monopoles 1 and 2 far electric fields, $\mathrm{E}_{\theta 1}$ and $\mathrm{E}_{\theta 2}$, which are given by [22], [23]

$$\mathrm{E}_{\theta \mathrm{i}} = \mathrm{j}\,60\,\mathrm{I_i}\,\beta\mathrm{H_{ei}}\,\frac{\mathrm{e}^{-\mathrm{j}\,\beta\,\mathrm{r}}}{\mathrm{r}}\,\sin\theta \qquad \mathrm{i} = 1,\ 2 \quad (29)$$

Where

r is the distance from the antenna to any point in space [m].
$\theta$ is the zenith angle.

The total far electric field, $\mathrm{E}_\theta = \mathrm{E}_{\theta 1} + \mathrm{E}_{\theta 2}$, will be

$$\mathrm{E}_\theta \;=\; \mathrm{j}\,60\;(\,\mathrm{I}_1\,\beta\mathrm{H}_{\mathrm{e}1} + \mathrm{I}_2\,\beta\mathrm{H}_{\mathrm{e}2})\;\frac{\mathrm{e}^{-\mathrm{j}\,\beta\,\mathrm{r}}}{\mathrm{r}}\;\sin\theta \qquad (30)$$

Then

$$|\;\mathrm{E}_\theta\;| = \;60\;|\;\mathrm{I}_1\;|\;\;\beta\mathrm{H}_{\mathrm{e}}\;\frac{\sin\theta}{\mathrm{r}} \qquad (31)$$

Where the CFA effective height $\mathrm{H}_{\mathrm{e}}$ is defined as

$$\mathrm{H}_{\mathrm{e}} \;=\; \mathrm{H}_{\mathrm{e}1}\;\left|1 \;+\; \frac{\mathrm{I}_2\,\mathrm{H}_{\mathrm{e}2}}{\mathrm{I}_1\,\mathrm{H}_{\mathrm{e}1}}\right| \qquad (32)$$

Therefore, the CFA radiation resistance referred to monopole 1 can be defined as

$$\mathrm{R}_{\mathrm{rad}} \;=\; 40\;(\beta\mathrm{H}_{\mathrm{e}})^2 \qquad (33)$$

or

$$\mathrm{R}_{\mathrm{rad}} \;=\; 40\;(\beta\mathrm{H}_{\mathrm{e}1})^2\;\left|1 \;+\; \frac{\mathrm{I}_2\,\mathrm{H}_{\mathrm{e}2}}{\mathrm{I}_1\,\mathrm{H}_{\mathrm{e}1}}\right|^2 \qquad (34)$$

It is very important to understand that this radiation resistance is not the input resistance in any of the antenna ports and it depends on the current and effective height relationships of both monopoles.

The antenna radiated power can be calculated as

$$\mathrm{W}_{\mathrm{rad}} \;=|\;\mathrm{I}_1\;|^2\;\;\mathrm{R}_{\mathrm{rad}} \qquad (35)$$

Then, monopole 1 effective input current $|\mathrm{I}_1|$, for a given radiated power $\mathrm{W}_{\mathrm{rad}}$, becomes

$$|\;\mathrm{I}_1\;| = \sqrt{\frac{\mathrm{W}_{\mathrm{rad}}}{\mathrm{R}_{\mathrm{rad}}}} \qquad (36)$$

Equations (31), (33) and (36) give the following far effective electric field:

$$|\;\mathrm{E}_\theta\;| = \;\frac{\sqrt{30\,\mathrm{W}_{\mathrm{rad}}\,\mathrm{D}}}{\mathrm{r}}\;\;\sin\theta \qquad (37)$$

Thus, the CFA antenna directivity is $\mathrm{D} = 3$ due to the $\sin\theta$ far field radiation pattern, as given by any short monopole of height less than $0.1\lambda$, as was confirmed by antenna pattern measurements using a model [6].

Taking into account the antenna efficiency $\eta$, the radiated power $\mathrm{W}_{\mathrm{rad}}$ and gain G are given by [26]

$$\mathrm{W}_{\mathrm{rad}} \;=\; \eta\,\mathrm{W}_{\mathrm{in}} \qquad (38)$$

$$\mathrm{G} \;=\; \eta\,\mathrm{D} \qquad (39)$$

Then, the CFA far effective electric field becomes

$$|\;\mathrm{E}_\theta\;| = \;\frac{\sqrt{30\,\mathrm{W}_{\mathrm{in}}\,\mathrm{G}}}{\mathrm{r}}\;\;\sin\theta \qquad (40)$$

This equation is exactly the same as for any standard short monopole. This field is the non attenuated radiated electric field, because it depends only on the inverse distance law. The actual field intensity along the earth is affected by the soil physical constants and the diffraction due to the spherical earth [28], [29].

## IV. Antenna Tuning and Losses

In the antenna circuit there are losses in conductors, insulators, tuning system and in the earth surface within a circle half-wavelength in radius. In general, insulator losses are very low compared to the other and can be neglected.

In order to tune the antenna, a coil is connected in series to each port, obtaining real input impedances. These coils have merit factors given by

$$\mathrm{Q}_{\mathrm{Li}} = \frac{\mathrm{X}_{\mathrm{Li}}}{\mathrm{R}_{\mathrm{Li}}} \qquad \mathrm{i} = 1,\;2 \qquad (41)$$

Where $\mathrm{R}_{\mathrm{Li}}$ and $\mathrm{X}_{\mathrm{Li}}$ are the i-th monopole tuning coil resistance and reactance, respectively.

Network parameters can be written in the following way when losses and tuning coils are present:

$$\mathrm{Z}_{\mathrm{ii}} = \mathrm{Z}_{\mathrm{ii}}^{\infty} + \mathrm{R}_{\mathrm{ci}} + \mathrm{R}_{\mathrm{gpi}} + \mathrm{R}_{\mathrm{Li}} + \mathrm{j}\,\mathrm{X}_{\mathrm{Li}} \qquad \mathrm{i} = 1,\;2 \qquad (42)$$

$$\mathrm{Z}_{12} = \mathrm{Z}_{21} = \mathrm{R}_{12} \;+\; \mathrm{j}\,\mathrm{X}_{12} \qquad (43)$$

Where

$\mathrm{Z}_{\mathrm{ii}}^{\infty} \;=\; \mathrm{R}_{\mathrm{radi}} + \mathrm{j}\,\mathrm{X}_{\mathrm{ii}}$ is the i-th monopole self-impedance with no losses and no tuning coils [$\Omega$].

$\mathrm{R}_{\mathrm{radi}}$ is the i-th monopole radiation resistance [$\Omega$].

$\mathrm{R}_{\mathrm{ci}}$ is the i-th monopole conductor resistance [$\Omega$].

$\mathrm{R}_{\mathrm{gpi}}$ is the ground plane loss resistance due to the i-th monopole current distribution and soil conditions [$\Omega$].

The mutual resistance $\mathrm{R}_{12}$ and all the reactances are practically not affected by the antenna losses, because they depend on the very near field distribution, which is not appreciably affected by the finite soil conductivity [30], [31].

The CFA equivalent network with losses and tuning coils can be seen in Fig. 9.

### A. Conductor Loss Resistance

Conductor loss resistance $\mathrm{R}_{\mathrm{c}1}$, due to monopole 1 conductors, can be calculated using the following expression, determined from the current distribution on the monopole structure and its top-load [1]:

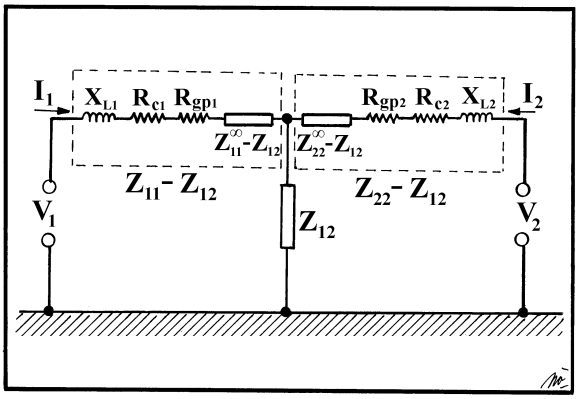


Fig. 9. CFA equivalent network with losses and tuning coils.

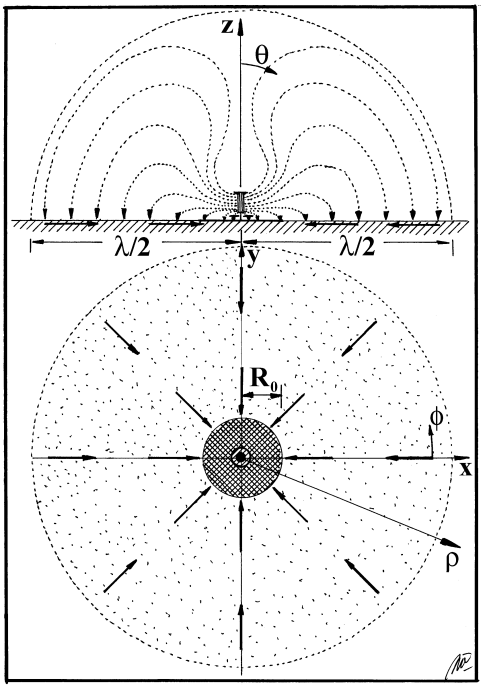


Fig. 10. CFA near electric field lines (displacement current) and ground plane surface conductive currents.

$$R_{c1} = \frac{R_{cL1}}{2}\left\{\left(1+\frac{X_{11}^2}{Z_{0m1}^2}\right)H_1 + \left(1-\frac{X_{11}^2}{Z_{0m1}^2}\right)\frac{\sin 2\beta H_1}{2\beta} + \frac{X_{11}}{Z_{0m1}}\frac{1-\cos 2\beta H_1}{\beta} + \frac{1}{n}\left(\cos\beta H_1 + \frac{X_{11}}{Z_{0m1}}\sin\beta H_1\right)^2 \left[L_1\left(1+\frac{1}{\tan^2\beta L_1}\right) + \frac{\sin 2\beta L_1}{2\beta}\left(1-\frac{1}{\tan^2\beta L_1}\right) + \frac{\cos 2\beta L_1 - 1}{\beta\tan\beta L_1}\right]\right\} \quad (44)$$

Where

$R_{cL1}$ is the monopole 1 wire resistance per unit length [$\Omega$/m].

$X_{11}$ is the monopole 1 self-reactance [$\Omega$].

$Z_{0m1}$ is the monopole 1 average characteristic impedance [$\Omega$].

$H_1$ is the monopole 1 height [m].

$L_1$ is the monopole 1 top-load length [m].

n is the number of the monopole 1 top-load branches.

The current distribution of the top-loaded monopole has been determined in [1] and can be seen in Fig. 4.

Conductor resistance per unit length, taking into account the skin effect, is given by [26]

$$R_{cL1} = \frac{1}{a_1}\sqrt{\frac{f\,\mu_0}{4\,\pi\,\sigma_c}} \quad (45)$$

Where

$\sigma_c$ is the conductor conductivity [S/m].

$a_1$ is the wire radius [m].

f is the operation frequency [Hz].

If the disk radius $L_2$ is sufficiently smaller than the wavelength, a linear current distribution over the disk can be assumed, as shown in Fig. 5, therefore

$$I(\rho) = I_2\,\frac{L_2 - \rho}{L_2 - r_h} \qquad r_h \le \rho \le L_2 \quad (46)$$

Where

$I(\rho)$ is the current distribution over the disk [A].

$I_2$ is the effective current at the disk center [A].

$L_2$ is the disk radius [m].

$r_h$ is the disk hole radius [m].

The disk feeding lead has a constant current distribution like a Hertz monopole ($I(z) = I_2$ in Fig. 5). From the disk and feeding lead current distributions, the monopole 2 conductor resistance, $R_{c2}$, can be calculated (see Appendix A), therefore

$$R_{c2} = R_{cL2}\,H_2 + \frac{1}{4\pi\,(L_2 - r_h)^2}\sqrt{\frac{\omega\,\mu_0}{2\,\sigma_c}} \left[L_2^2\,\ln\left(\frac{L_2}{r_h}\right) - 2\,L_2\,(L_2 - r_h) + \frac{L_2^2 - r_h^2}{2}\right] \quad (47)$$

The feeding lead conductor resistance per unit length, $R_{cL2}$, is given by (45) with subscript 2 instead of 1.

### *B. Ground Plane Loss Resistance*

The artificial ground plane [32] is made up by means of a circular metallic layer $R_0$ in radius with a small surface resistance $R_g$. Then, the ground plane equivalent loss resistance for each monopole is given by [1]

$$R_{gpi} = \frac{2\,\pi}{|I_i|^2}\left(\int_0^{R_0}|H_{\phi i}|^2\,R_g\,\rho\,d\rho + \int_{R_0}^{\lambda/2}|H_{\phi i}|^2\,R_s\,\rho\,d\rho\right) \quad (48)$$

Where $i = 1,\ 2$ and

$R_{gpi}$ is the i-th monopole ground plane loss resistance [$\Omega$].

$H_{\phi i}$ is the i-th monopole near magnetic field on the ground surface, given by (21) [A/m].

$R_g$ is the surface resistance of the artificial ground plane or metallic layer, given by (25) [$\Omega$].

$R_s$ is the surface resistance of the natural ground plane or soil, given by (27) [$\Omega$].

Fig. 10 shows a sketch of the displacement currents and the conductive currents flowing on the ground plane at a specific time.

The ground plane is considered up to a distance $\rho = \lambda/2$ because this is the maximum distance covered by the ground surface currents under the antenna, closing the antenna electric circuit. Beyond this distance, the ground currents do not return to the antenna generators and are taken into account in the surface wave propagation calculations [1].

## V. Efficiency and Gain

Antenna efficiency $\eta$ is defined as the ratio between the radiated power $W_{rad}$ and the input power $W_{in}$. The power radiated by the CFA antenna is given by (35), while the antenna input power can be written as

$$W_{in} = | I_1 |^2 \, R_1 + | I_2 |^2 \, R_2 \tag{49}$$

Where $R_i$ is the i-th port input resistance, $i = 1,\ 2$.

Then, the CFA efficiency will be

$$\eta = \frac{R_{rad}}{R_1 + | I_2/I_1 |^2 \, R_2} \tag{50}$$

Where

$$\left| \frac{I_2}{I_1} \right|^2 = K^2 \left| \frac{Z_1}{Z_2} \right|^2 \tag{51}$$

and the input impedances $Z_1$ and $Z_2$ are given by (16) and (17), respectively.

It can be seen that the CFA efficiency $\eta$ depends on the antenna geometry, operation frequency, the voltage amplitude ratio K and the phase difference $\phi_2$.

Antenna gain, taking into account the directivity $D = 3$, is $G = \eta D = 3\,\eta$.

## VI. Bandwidth

The CFA antenna has two ports, for this reason, two bandwidths can be defined, according to the reflection coefficients of both ports. In this case, taking into account that both input powers, $W_1$ and $W_2$, must be positive, it is more convenient to define a CFA average reflection coefficient as a weighted geometric mean of the reflection coefficients, $\Gamma_1$ and $\Gamma_2$, of both ports. Thus, the CFA average reflection coefficient is given by

$$| \Gamma | = \sqrt{\frac{W_1 \, | \Gamma_1 |^2 + W_2 \, | \Gamma_2 |^2}{W_{in}}} \tag{52}$$

Then, the CFA VSWR will be

$$VSWR = \frac{1 + | \Gamma |}{1 - | \Gamma |} \tag{53}$$

TABLE I

CFA dimensions in meters.

| | | |
|---|---|---|
| Monopole 1 height | $H_1$ | 10 |
| Barrel diameter | $D_1$ | 3.0 |
| Monopole 1 top-load length | $L_1$ | 0.0 |
| Barrel base height | $\delta_1$ | 1.5 |
| Monopole 1 wire radius | $a_1$ | $6 \cdot 10^{-3}$ |
| Monopole 2 (disk) height | $H_2$ | 1.0 |
| Disk radius (monopole 2 top-load length) | $L_2$ | 2.5 |
| Disk hole radius | $r_h$ | 0.05 |
| Monopole 2 wire radius | $a_2$ | $6 \cdot 10^{-3}$ |
| Artificial ground plane radius | $R_0$ | 5.0 |

TABLE II

CFA equivalent network matrix.

| METHOD | $Z_{11}$ | $Z_{12}$ | $Z_{22}$ |
|---|---|---|---|
| **TLM** | $2.18 - j\,410$ | $0.11 - j\,124$ | $0.09 - j\,856$ |
| **MoM** | $2.13 - j\,430$ | $0.20 - j\,117$ | $0.13 - j\,844$ |

## VII. Examples

Having the available theory expressed previously, the Crossed Field Antenna analysis can be made by means of numerical examples.

### A. CFA Operating Windows

As a first example, a CFA model is analyzed at the frequency of 1 MHz, with the antenna dimensions indicated in Table I and over average soil ($\sigma = 10^{-2}$ S/m, $\epsilon_r = 10$).

The CFA equivalent network impedance matrix can be calculated using the Transmission Line Method (TLM) and by means of the Method of Moments (MoM) [33] (wire grid model [25]). Both methods produce practically the same result, as can be seen in Table II for 1 MHz and average ground.

In this example, monopole 1 is a barrel build up by twenty four copper wires ($\sigma_c = 5.8 \cdot 10^7$ S/m) of radius $a_1$, as shown in Fig. 4. Barrel diameter, $D_1$, wire radius, $a_1$, and barrel base height, $\delta_1$, are taken into account in the calculation of the monopole 1 equivalent transmission line average characteristic impedance $Z_{0m1}$ [1].

As a first analysis, input impedances of both antenna ports are calculated as functions of voltage phase difference $\phi_2$ for $K = 1$ and over average ground, and can be seen in Figs. 11 and 12.

In Fig. 11, negative input resistances $R_1$ and $R_2$ can be seen for some ranges of $\phi_2$, while in Fig. 12 the input reactances $X_1$ and $X_2$ are always negative. There exist two small windows, difficult to appreciate in Fig. 11, where both input resistances are positive, permitting the antenna operation. One window is located in the neighborhood of $\phi_2 = 180°$ and the other near $\phi_2 = 360°$.

Input impedances are shown in both windows in Tables III and IV. It is interesting to see that the input reactances are practically constant in both windows, where the antenna can operate.

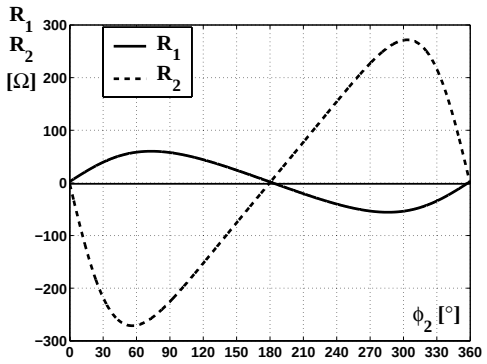


Fig. 11. CFA input resistances $\mathrm{R}_1$ and $\mathrm{R}_2$ as functions of $\phi_2$ for $\mathrm{K} = 1$ and over average ground.

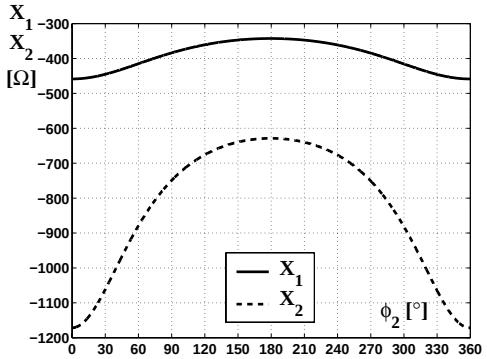


Fig. 12. CFA input reactances $\mathrm{X}_1$ and $\mathrm{X}_2$ as functions of $\phi_2$ for $\mathrm{K} = 1$ and over average ground.

TABLE III

CFA INPUT IMPEDANCES IN $180°$-WINDOW.

| $\phi_2$ | $\mathrm{R}_1$ | $\mathrm{X}_1$ | $\mathrm{R}_2$ | $\mathrm{X}_2$ |
|---|---|---|---|---|
| deg | $\Omega$ | $\Omega$ | $\Omega$ | $\Omega$ |
| 179.4 | 2.30 | $-343$ | $-0.71$ | $-629$ |
| 179.8 | 2.00 | $-343$ | 0.31 | $-629$ |
| 180.2 | 1.70 | $-343$ | 1.32 | $-629$ |
| 180.6 | 1.39 | $-343$ | 2.34 | $-629$ |
| 181.0 | 1.09 | $-343$ | 3.36 | $-629$ |
| 181.4 | 0.79 | $-343$ | 4.37 | $-629$ |
| 181.8 | 0.49 | $-343$ | 5.39 | $-629$ |
| 182.2 | 0.19 | $-343$ | 6.41 | $-629$ |
| 182.6 | $-0.12$ | $-343$ | 7.42 | $-629$ |

TABLE IV

CFA INPUT IMPEDANCES IN $360°$-WINDOW.

| $\phi_2$ | $\mathrm{R}_1$ | $\mathrm{X}_1$ | $\mathrm{R}_2$ | $\mathrm{X}_2$ |
|---|---|---|---|---|
| deg | $\Omega$ | $\Omega$ | $\Omega$ | $\Omega$ |
| 358.0 | $-0.12$ | $-459$ | 15.7 | $-1171$ |
| 358.2 | 0.15 | $-459$ | 14.0 | $-1171$ |
| 358.4 | 0.42 | $-459$ | 12.2 | $-1171$ |
| 358.6 | 0.69 | $-459$ | 10.4 | $-1172$ |
| 358.8 | 0.96 | $-459$ | 8.67 | $-1172$ |
| 359.0 | 1.23 | $-459$ | 6.90 | $-1172$ |
| 359.2 | 1.50 | $-459$ | 5.14 | $-1172$ |
| 359.4 | 1.77 | $-459$ | 3.37 | $-1172$ |
| 359.6 | 2.04 | $-459$ | 1.61 | $-1172$ |
| 359.8 | 2.31 | $-459$ | $-0.16$ | $-1172$ |

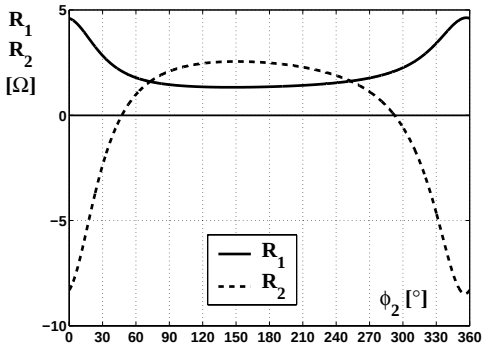


Fig. 13. Tuned CFA input resistances $\mathrm{R}_1$ and $\mathrm{R}_2$ as functions of $\phi_2$ for $\mathrm{K} = 1$. The $180°$-window can clearly be seen where $\mathrm{R}_1$ and $\mathrm{R}_2$ are positive.

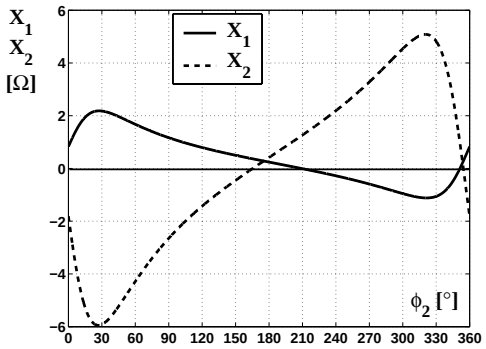


Fig. 14. Tuned CFA input reactances $\mathrm{X}_1$ and $\mathrm{X}_2$ as functions of $\phi_2$ for $\mathrm{K} = 1$ and in the $180°$-window.

In order to tune the antenna, opposite reactances are connected in series to both ports. If the $180°$-window is chosen, the reactance to be connected in series with port 1 is $\mathrm{X}_{\mathrm{L}1} = 343\ \Omega$ and with port 2 is $\mathrm{X}_{\mathrm{L}2} = 629\ \Omega$. Under this condition, the input resistances and reactances of both ports are shown in Figs. 13 and 14, where they have a very small variation as functions of $\phi_2$, also the input impedances of both ports are practically real close to $\phi_2 = 180°$. In this example, only the antenna losses are taken into account and the tuning coils are supposed to be of infinite merit factor $\mathrm{Q}_{\mathrm{L}} = \mathrm{Q}_{\mathrm{L}1} = \mathrm{Q}_{\mathrm{L}2}$, permitting to know the antenna operation without any other effect.

In the $180°$-window, when the generators have the same voltage amplitude ($\mathrm{K} = 1$), the antenna is operational because the input powers on both ports are positive for $\phi_2$ between $50°$ and $290°$, where both input resistances are positive. In this case, the equivalent network mutual conductance is negative, $\mathrm{G}_{12} = -0.253$ S, and the antenna operates as in Fig. 7.

If the $360°$-window is chosen, the reactance to be connected in series with port 1 is $\mathrm{X}_{\mathrm{L}1} = 459\ \Omega$ and with port 2 is $\mathrm{X}_{\mathrm{L}2} = 1172\ \Omega$. Under this condition, the input resistances and reactances of both ports are shown in Figs. 15 and 16, where they also have a very small variation as functions of $\phi_2$. The input impedances of both ports are practically real for $\phi_2$ between $0°$ and $100°$ and between $240°$ and $360°$. In this case, the antenna is operational too, because the input powers in both ports are positive. Also, because the equivalent network mutual conductance is positive, $\mathrm{G}_{12} = 0.165$ S, the

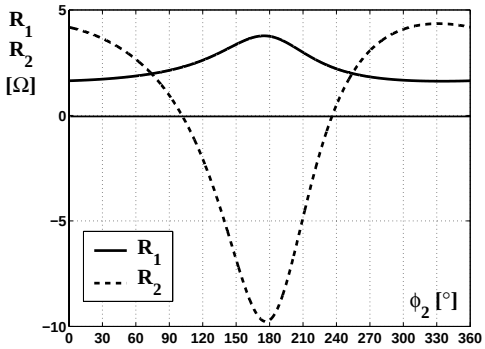


Fig. 15. Tuned CFA input resistances $\mathrm{R}_1$ and $\mathrm{R}_2$ as functions of $\phi_2$ for $\mathrm{K} = 1$. The $360°$-window can clearly be seen where $\mathrm{R}_1$ and $\mathrm{R}_2$ are positive.

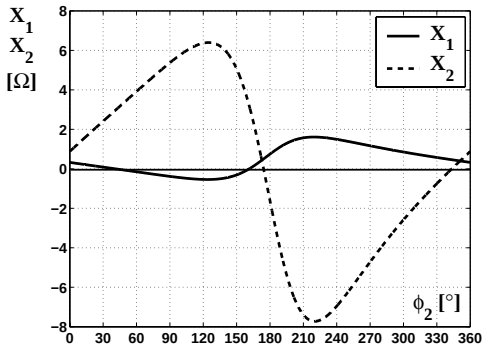


Fig. 16. Tuned CFA input reactances $\mathrm{X}_1$ and $\mathrm{X}_2$ as functions of $\phi_2$ for $\mathrm{K} = 1$ and in the $360°$-window.

antenna operates as in Fig. 6.

From this analysis, the range of the voltage phase difference $\phi_2$ was obtained under antenna resonance condition, when the input impedances of both ports are practically real or resistive.

The $\phi_2$ value of interest in these ranges or windows is that which permits to have the input powers, $\mathrm{W}_1$ and $\mathrm{W}_2$, under control, with a given relationship $\mathrm{K_w} = \mathrm{W}_2/\mathrm{W}_1$.

In some cases, it is possible to find values of K, $\phi_2$ and $\mathrm{V}_1$, which permit to get a given total input power, $\mathrm{W_{in}} = \mathrm{W}_1 + \mathrm{W}_2$, and a given power ratio $\mathrm{K_w} = \mathrm{W}_2/\mathrm{W}_1$, under the conditions $\mathrm{W}_1 > 0$ and $\mathrm{W}_2 > 0$. In other words, generator voltages $\mathrm{V}_1$ and $\mathrm{V}_2$ can be adjusted to give a specified total input power and power ratio, but this is not always possible. In Appendix B, it is found that if $\phi_2$ is written as a function of K, and K satisfies a certain condition, then a solution is possible.

### *B. CFA Performance*

Knowing the CFA operation in both windows, input impedances, near field, wave impedance, radiation resistance, efficiency, gain and far field strength at 1 km for 1 kW input power can be calculated.

In Tables V and VI, the results of the CFA $180°$ and $360°$-windows can be seen.

A monopole with the same height ($\mathrm{H}_1/\lambda = 0.0333$), taken as reference, has a radiation resistance $\mathrm{R_{rad}} = 0.71\ \Omega$, a gain $\mathrm{G} = -0.12$ dBi and the corresponding field strength at 1 km for 1 kW of input power is $\mathrm{E} = 171$ mV/m. The CFA has

TABLE V
CFA PERFORMANCE IN $180°$-WINDOW.

| K | $\phi_2$ | $\mathrm{R}_1$ | $\mathrm{X}_1$ | $\mathrm{R}_2$ | $\mathrm{X}_2$ | $\mathrm{R_{rad}}$ |
|---|---|---|---|---|---|---|
| – | deg | Ω | Ω | Ω | Ω | Ω |
| 1.6 | 130.6 | 1.04 | 0.68 | 3.47 | −1.08 | 0.59 |
| 1.7 | 155.3 | 1.04 | 0.42 | 3.50 | −0.22 | 0.59 |
| 1.8 | 174.4 | 1.04 | 0.24 | 3.52 | 0.40 | 0.59 |
| 1.9 | 191.9 | 1.04 | 0.07 | 3.54 | 0.95 | 0.60 |
| 2.0 | 209.6 | 1.05 | −0.10 | 3.55 | 1.53 | 0.60 |
| 2.1 | 230.3 | 1.05 | −0.32 | 3.58 | 2.28 | 0.60 |

| K | $\mathrm{V}_1$ | $\lvert\mathrm{V}_2\rvert$ | $\lvert\mathrm{I}_1\rvert$ | $\lvert\mathrm{I}_2\rvert$ | G | E |
|---|---|---|---|---|---|---|
| – | V | V | A | A | dBi | mV/m |
| 1.6 | 27.3 | 43.6 | 21.9 | 12.0 | −0.69 | 160 |
| 1.7 | 24.7 | 41.9 | 21.9 | 12.0 | −0.69 | 160 |
| 1.8 | 23.4 | 42.2 | 21.9 | 11.9 | −0.69 | 160 |
| 1.9 | 22.9 | 43.5 | 21.9 | 11.9 | −0.68 | 160 |
| 2.0 | 23.0 | 45.9 | 21.9 | 11.9 | −0.68 | 160 |
| 2.1 | 23.9 | 50.2 | 21.9 | 11.8 | −0.68 | 160 |

TABLE VI
CFA PERFORMANCE IN $360°$-WINDOW.

| K | $\phi_2$ | $\mathrm{R}_1$ | $\mathrm{X}_1$ | $\mathrm{R}_2$ | $\mathrm{X}_2$ | $\mathrm{R_{rad}}$ |
|---|---|---|---|---|---|---|
| – | deg | Ω | Ω | Ω | Ω | Ω |
| 2.2 | 310.1 | 1.14 | 0.77 | 7.57 | −1.96 | 0.79 |
| 2.4 | 341.3 | 1.14 | 0.42 | 7.46 | 0.37 | 0.79 |
| 2.6 | 4.873 | 1.14 | 0.18 | 7.39 | 1.96 | 0.80 |
| 2.8 | 27.48 | 1.14 | −0.06 | 7.32 | 3.50 | 0.80 |
| 3.0 | 54.52 | 1.14 | −0.38 | 7.22 | 5.51 | 0.80 |

| K | $\mathrm{V}_1$ | $\lvert\mathrm{V}_2\rvert$ | $\lvert\mathrm{I}_1\rvert$ | $\lvert\mathrm{I}_2\rvert$ | G | E |
|---|---|---|---|---|---|---|
| – | V | V | A | A | dBi | mV/m |
| 2.2 | 28.9 | 63.5 | 20.9 | 8.13 | 0.18 | 177 |
| 2.4 | 25.5 | 61.1 | 20.9 | 8.19 | 0.19 | 177 |
| 2.6 | 24.2 | 62.9 | 20.9 | 8.23 | 0.19 | 177 |
| 2.8 | 23.9 | 67.0 | 20.9 | 8.27 | 0.19 | 177 |
| 3.0 | 25.2 | 75.6 | 20.9 | 8.32 | 0.19 | 177 |

the same 1 kW input power with 500 W applied to each port ($\mathrm{K_w} = 1$ and $\mathrm{W}_1 = \mathrm{W}_2 = 500$ W).

From the two CFA operating windows, in Tables V and VI, a small loss (0.57 dB) and a small gain (0.31 dB) can be seen with respect to the gain of the reference monopole.

The CFA and reference monopole VSWR have been calculated for average ground at the center frequency of 1 MHz, for a metallic ground plane 5 m in radius, for $\mathrm{K} = 1.8$ and $\phi_2 = 174.4°$ ($180°$-window) in Fig. 17 and for $\mathrm{K} = 2.4$ and $\phi_2 = 341.3°$ ($360°$-window) in Fig. 18. The VSWR sharp behavior is due to a very low antenna height in both cases ($\mathrm{H}_1/\lambda = 0.0333$).

At the center frequency of 1 MHz, the input power in each port is exactly 500 W, then the total input power is 1 kW. As frequency is increased or decreased, the input powers in both ports are not exactly equal and this difference is higher at the minimum and maximum frequencies of the useful bandwidth.

It can be noticed from these calculations that the CFA bandwidth is a little bit better in the $180°$-window, but the

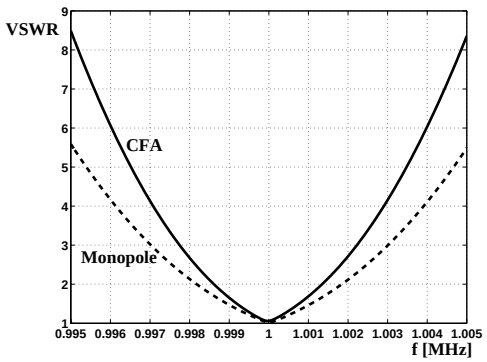


Fig. 17. CFA and monopole VSWR as a function of frequency for $\mathrm{K} = 1.8$ and $\phi_2 = 174.4°$.

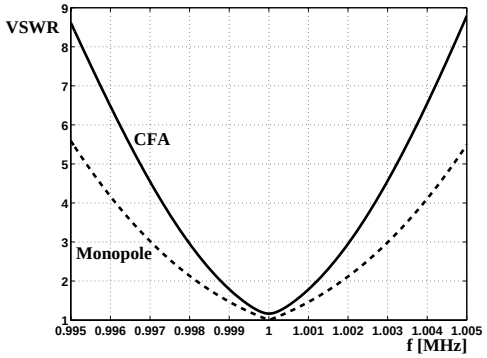


Fig. 18. CFA and monopole VSWR as a function of frequency for $\mathrm{K} = 2.4$ and $\phi_2 = 341.3°$.

antenna gain is a little bit lower. This difference is theoretically noticeable but it is not really significant from the engineering point of view. Furthermore, a monopole of the same height has a similar gain and more bandwidth as calculations indicate, but it is more convenient in practice due to an easier system to be tuned.

### *C. Tuning Coil Losses*

Tuning coil losses are included for several merit factors $\mathrm{Q_L} = \mathrm{Q_{L1}} = \mathrm{Q_{L2}}$, in order to know their effects on the antenna performance. These losses are also included in the reference monopole of height $\mathrm{H_1}/\lambda = 0.0333$.

In Table VII, the effect of the tuning coil merit factor $\mathrm{Q_L}$ is clearly seen in the monopole behavior when it is placed on an average ground. Antenna bandwidth has been calculated for $\mathrm{VSWR} = 2$ and electric field strength at 1 km corresponds to an input power of 1 kW.

The same effect is seen in Tables VIII and IX for the CFA when it is operating in the $180°$- and $360°$-windows.

When losses are increased, a corresponding increase in the antenna bandwidth is clearly obtained. Nevertheless, a decrease in gain occurs for the monopole and CFA in both windows.

### *D. Near Field*

With the tuning coil losses taken into account, for a merit factor $\mathrm{Q_L} = 200$, near electric and magnetic fields have been calculated for both windows and, specifically, for $\mathrm{K} = 1.8$ and $\phi_2 = 174.4°$ (Table V) and for $\mathrm{K} = 2.4$ and $\phi_2 = 341.3°$ (Table VI). In Fig. 19, the near electric field for the CFA and the reference monopole over average ground can be seen as a function of distance, for an input power of 1 kW.

The ratio between the near electric and magnetic fields is the wave impedance $\mathrm{Z_0}$ as a function of distance $\rho/\lambda$ and it can be seen in Fig. 20. This wave impedance is practically the same for both CFA windows, so only one curve for magnitude and one for phase are presented in Fig. 20.

In Table X, wave impedances are calculated for the CFA and a reference monopole of the same height ($\mathrm{H_1}/\lambda = 0.0333$), at a frequency of 1 MHz and over average ground. The Moment Method solution is very close to the values given here.

**It can be noticed that the CFA wave impedance is very close to that of the reference monopole. Furthermore, no Poynting Vector Synthesis (PVS) [34] can be seen, because the wave impedance is reactive close to the antenna and real at distances greater than half-wavelength ($\mathrm{Z_0} \cong 377\ \Omega$). Therefore, the CFA behaves like any short monopole, because a reactive near field zone exists close to the antenna structure and the radiated field starts at a distance near to half-wavelength.**

TABLE VII
SHORT MONOPOLE TUNING COIL EFFECT.

| $\mathrm{Q_L}$ | $\pm\Delta$f | $\eta$ | G | E | E |
|---|---|---|---|---|---|
| – | kHz | – | dBi | mV/m | dB$\mu$V/m |
| $\infty$ | 1.8 | 0.32 | $-0.12$ | 171 | 104.65 |
| 400 | 2.7 | 0.22 | $-1.80$ | 141 | 102.98 |
| 200 | 3.5 | 0.17 | $-3.00$ | 123 | 101.77 |
| 100 | 5.2 | 0.11 | $-4.71$ | 101 | 100.06 |
| 50 | 8.7 | 0.07 | $-6.90$ | 78.3 | 97.88 |

TABLE VIII
$180°$-WINDOW CFA TUNING COIL EFFECT.

| $\mathrm{Q_L}$ | $\pm\Delta$f | $\eta$ | G | E | E |
|---|---|---|---|---|---|
| – | kHz | – | dBi | mV/m | dB$\mu$V/m |
| $\infty$ | 1.4 | 0.28 | $-0.69$ | 160 | 104.09 |
| 400 | 2.2 | 0.17 | $-2.82$ | 125 | 101.95 |
| 200 | 3.1 | 0.13 | $-4.24$ | 106 | 100.53 |
| 100 | 4.8 | 0.08 | $-6.18$ | 85.1 | 98.59 |
| 50 | 8.2 | 0.05 | $-8.54$ | 64.8 | 96.24 |

TABLE IX
$360°$-WINDOW CFA TUNING COIL EFFECT.

| $\mathrm{Q_L}$ | $\pm\Delta$f | $\eta$ | G | E | E |
|---|---|---|---|---|---|
| – | kHz | – | dBi | mV/m | dB$\mu$V/m |
| $\infty$ | 1.2 | 0.35 | 0.19 | 177 | 104.96 |
| 400 | 2.1 | 0.20 | $-2.11$ | 136 | 102.66 |
| 200 | 2.9 | 0.15 | $-3.61$ | 114 | 101.16 |
| 100 | 4.7 | 0.09 | $-5.59$ | 91.0 | 99.18 |
| 50 | 8.1 | 0.05 | $-7.98$ | 69.1 | 96.79 |

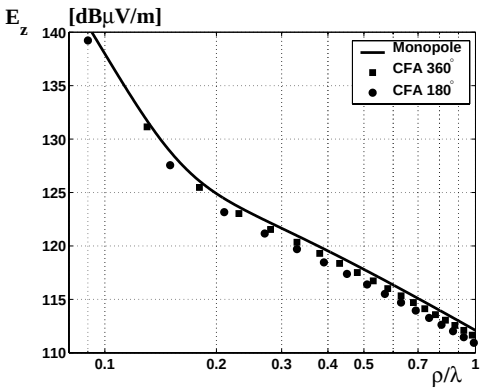


Fig. 19. CFA near electric field $E_z$ as a function of distance $\rho/\lambda$ at 1 MHz for average ground ($\sigma = 10^{-2}$ S/m, $\epsilon_r = 10$) and an input power of 1 kW.

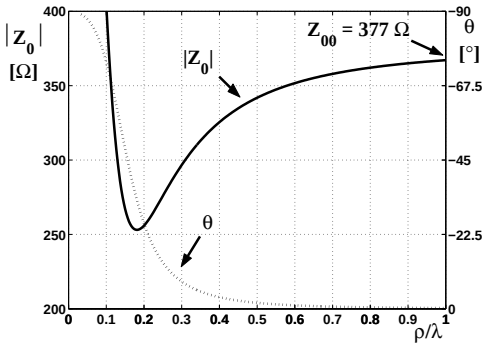


Fig. 20. CFA wave impedance as a function of distance $\rho/\lambda$ at 1 MHz.

TABLE X
CFA AND SHORT MONOPOLE WAVE IMPEDANCES.

| $\rho/\lambda$ | $\lvert Z_{0\,CFA} \rvert$ | $\theta_{CFA}$ | $\lvert Z_{0\,MON} \rvert$ | $\theta_{MON}$ |
|---|---|---|---|---|
| – | Ω | ∘ | Ω | ∘ |
| 0.1 | 387.7 | −73.9 | 385.5 | −73.8 |
| 0.2 | 254.9 | −25.4 | 254.8 | −25.3 |
| 0.3 | 296.5 | −8.14 | 296.4 | −8.12 |
| 0.4 | 325.4 | −3.47 | 325.3 | −3.47 |
| 0.5 | 341.8 | −1.79 | 341.8 | −1.78 |
| 0.6 | 351.6 | −1.04 | 351.6 | −1.03 |
| 0.7 | 357.9 | −0.65 | 357.9 | −0.65 |
| 0.8 | 362.1 | −0.44 | 362.1 | −0.44 |
| 0.9 | 365.0 | −0.31 | 365.0 | −0.31 |
| 1.0 | 367.1 | −0.22 | 367.1 | −0.22 |
| 2.0 | 374.1 | −0.03 | 374.1 | −0.03 |
| 3.0 | 375.4 | −0.01 | 375.4 | −0.01 |
| 4.0 | 375.9 | −0.00 | 375.9 | −0.00 |
| 5.0 | 376.1 | −0.00 | 376.1 | −0.00 |

TABLE XI
SHORT MONOPOLE OVER WET SOIL.

| $Q_L$ | $\pm\Delta f$ | $\eta$ | G | E | E |
|---|---|---|---|---|---|
| – | kHz | – | dBi | mV/m | dBμV/m |
| ∞ | 1.3 | 0.46 | 1.36 | 202 | 106.13 |
| 400 | 2.2 | 0.27 | −0.85 | 157 | 103.93 |
| 200 | 3.0 | 0.20 | −2.30 | 133 | 102.47 |
| 100 | 4.7 | 0.13 | −4.25 | 106 | 100.52 |
| 50 | 8.1 | 0.07 | −6.62 | 80.8 | 98.15 |

TABLE XII
180°-WINDOW CFA OVER WET SOIL.

| $Q_L$ | $\pm\Delta f$ | $\eta$ | G | E | E |
|---|---|---|---|---|---|
| – | kHz | – | dBi | mV/m | dBμV/m |
| ∞ | 1.0 | 0.41 | 0.90 | 192 | 105.67 |
| 400 | 1.8 | 0.21 | −1.92 | 139 | 102.85 |
| 200 | 2.7 | 0.15 | −3.61 | 114 | 101.16 |
| 100 | 4.4 | 0.09 | −5.78 | 89.0 | 98.99 |
| 50 | 7.8 | 0.05 | −8.31 | 66.5 | 96.46 |

### *E. Soil Effect*

Antenna performance has been calculated changing the type of soil. In Tables XI, XII and XIII the performance of a short monopole and a CFA of the same height ($H_1/\lambda = 0.0333$) operating in the 180°- and 360°-windows can be seen over wet soil ($\sigma = 0.03$ S/m and $\epsilon_r = 20$).

In Tables XIV, XV and XVI the performance of a short monopole and a CFA of the same height ($H_1/\lambda = 0.0333$) operating in the 180°- and 360°-windows can be seen over dry soil ($\sigma = 0.001$ S/m and $\epsilon_r = 4$).

Field strength E at 1 km corresponds to an input power of 1 kW. From these calculations, it can be noticed a better bandwidth for every case in favor of the short monopole. Also, an increase in bandwidth is achieved when tuning coil and

TABLE XIII
360°-WINDOW CFA OVER WET SOIL.

| $Q_L$ | $\pm\Delta f$ | $\eta$ | G | E | E |
|---|---|---|---|---|---|
| – | kHz | – | dBi | mV/m | dBμV/m |
| ∞ | 0.9 | 0.48 | 1.60 | 208 | 106.37 |
| 400 | 1.7 | 0.24 | −1.34 | 148 | 103.43 |
| 200 | 2.6 | 0.16 | −3.07 | 122 | 101.70 |
| 100 | 4.3 | 0.10 | −5.26 | 94.5 | 99.51 |
| 50 | 7.8 | 0.06 | −7.79 | 70.6 | 96.98 |

TABLE XIV
SHORT MONOPOLE OVER DRY SOIL.

| $Q_L$ | $\pm\Delta f$ | $\eta$ | G | E | E |
|---|---|---|---|---|---|
| – | kHz | – | dBi | mV/m | dBμV/m |
| ∞ | 4.7 | 0.12 | −4.26 | 106 | 100.51 |
| 400 | 5.6 | 0.11 | −4.98 | 97.6 | 99.79 |
| 200 | 6.4 | 0.09 | −5.60 | 90.9 | 99.17 |
| 100 | 8.1 | 0.07 | −6.63 | 80.8 | 98.15 |
| 50 | 11.5 | 0.05 | −8.15 | 67.8 | 96.62 |

TABLE XV

180°-WINDOW CFA OVER DRY SOIL.

| $Q_L$ | $\pm\Delta f$ | $\eta$ | G | E | E |
|---|---|---|---|---|---|
| – | kHz | – | dBi | mV/m | dB$\mu$V/m |
| $\infty$ | 3.6 | 0.11 | −4.98 | 97.6 | 99.79 |
| 400 | 4.4 | 0.09 | −5.90 | 87.8 | 98.87 |
| 200 | 5.3 | 0.07 | −6.66 | 80.4 | 98.11 |
| 100 | 6.9 | 0.05 | −7.87 | 70.0 | 96.90 |
| 50 | 10.3 | 0.04 | −9.61 | 57.3 | 95.17 |

TABLE XVI

360°-WINDOW CFA OVER DRY SOIL.

| $Q_L$ | $\pm\Delta f$ | $\eta$ | G | E | E |
|---|---|---|---|---|---|
| – | kHz | – | dBi | mV/m | dB$\mu$V/m |
| $\infty$ | 3.2 | 0.14 | −3.85 | 111 | 100.92 |
| 400 | 4.1 | 0.11 | −4.91 | 98.4 | 99.86 |
| 200 | 5.0 | 0.09 | −5.75 | 89.3 | 99.02 |
| 100 | 6.8 | 0.07 | −7.07 | 76.7 | 97.70 |
| 50 | 10.0 | 0.04 | −8.89 | 62.2 | 95.88 |

ground losses are increased.

### *F. Artificial Ground Plane Effect*

A circular metallic ground plane of radius $R_0$ and copper conductivity ($\sigma_m = 5.8 \cdot 10^7$ S/m) is laid down under the monopole and CFA antennas. The effect of this radius $R_0$ on the antenna performance over average ground is analyzed for tuning coils of merit factor $Q_L = 200$.

In Tables XVII, XVIII and XIX the short monopole, 180°- and 360°-window CFA performances are presented as functions of the artificial ground plane radius $R_0$, where field strength E at 1 km corresponds to an input power of 1 kW.

It can be appreciated from these results that the greater the ground plane radius $R_0$ the greater the antenna gain G and the smaller the bandwidth $\pm\Delta f$, which is a well known effect.

TABLE XVII

MONOPOLE PERFORMANCE OVER METALLIC GROUND PLANE.

| $R_0$ | $\pm\Delta f$ | $\eta$ | G | E | E |
|---|---|---|---|---|---|
| m | kHz | – | dBi | mV/m | dB$\mu$V/m |
| 5 | 3.5 | 0.17 | −3.00 | 123 | 101.77 |
| 10 | 2.8 | 0.21 | −2.05 | 137 | 102.72 |
| 20 | 2.5 | 0.23 | −1.53 | 145 | 103.24 |
| 30 | 2.4 | 0.24 | −1.38 | 148 | 103.39 |

TABLE XVIII

180°-WINDOW CFA PERFORMANCE OVER METALLIC GROUND PLANE.

| $R_0$ | $\pm\Delta f$ | $\eta$ | G | E | E |
|---|---|---|---|---|---|
| m | kHz | – | dBi | mV/m | dB$\mu$V/m |
| 5 | 3.1 | 0.13 | −4.24 | 106 | 100.53 |
| 10 | 2.6 | 0.15 | −3.39 | 117 | 101.38 |
| 20 | 2.3 | 0.17 | −2.94 | 124 | 101.84 |
| 30 | 2.2 | 0.17 | −2.81 | 125 | 101.97 |

TABLE XIX

360°-WINDOW CFA PERFORMANCE OVER METALLIC GROUND PLANE.

| $R_0$ | $\pm\Delta f$ | $\eta$ | G | E | E |
|---|---|---|---|---|---|
| m | kHz | – | dBi | mV/m | dB$\mu$V/m |
| 5 | 2.9 | 0.15 | −3.61 | 114 | 101.16 |
| 10 | 2.5 | 0.17 | −2.88 | 124 | 101.89 |
| 20 | 2.3 | 0.19 | −2.51 | 130 | 102.26 |
| 30 | 2.2 | 0.19 | −2.40 | 131 | 102.37 |

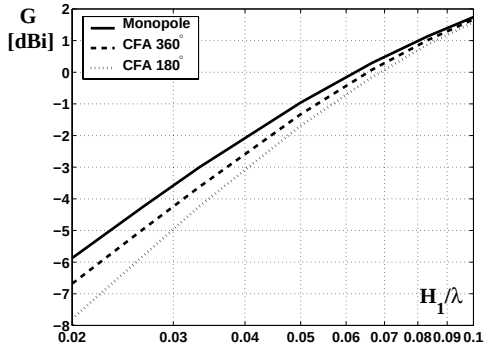


Fig. 21. CFA gain as a function of monopole 1 height $H_1/\lambda$, for a disk radius of $L_2 = 2.5$ m, at the frequency f = 1 MHz and over average ground.

### *G. Height Effect*

The CFA antenna performance has been analyzed as a function of the monopole 1 height, $H_1$, and with a constant disk radius of $L_2 = 2.5$ m over average ground and with tuning coils of merit factor $Q_L = 200$. A reference monopole of the same height has also been calculated.

Figs. 21 and 22 show the antenna gain and bandwidth as functions of height $H_1/\lambda$.

With regard to the antenna gain, Fig. 21 shows that the gain difference is smaller for greater antenna heights, this means that the disk has a deleterious effect on the antenna performance. At the same time, Fig. 22 shows a better bandwidth of the monopole compared to the CFA for any height.

### *H. Disk Effect*

The CFA antenna performance has been analyzed as a function of the disk radius, $L_2$, and with a constant monopole 1

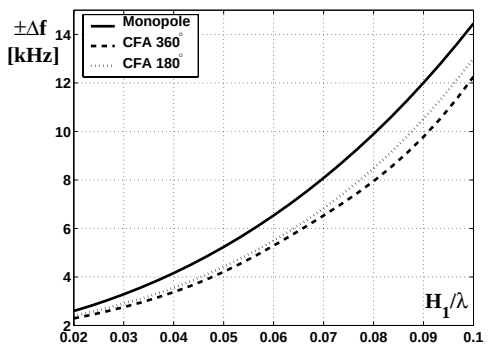


Fig. 22. CFA bandwidth for VSWR = 2 as a function of monopole 1 height $H_1/\lambda$, for a disk radius of $L_2 = 2.5$ m, at the center frequency f = 1 MHz and over average ground.

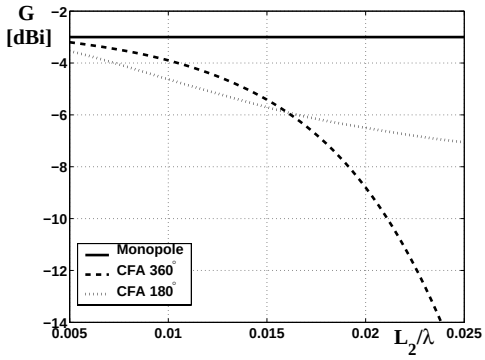


Fig. 23. CFA gain as a function of disk radius $L_2/\lambda$ for a monopole 1 height of $H_1 = 10$ m, at the frequency f = 1 MHz and over average ground.

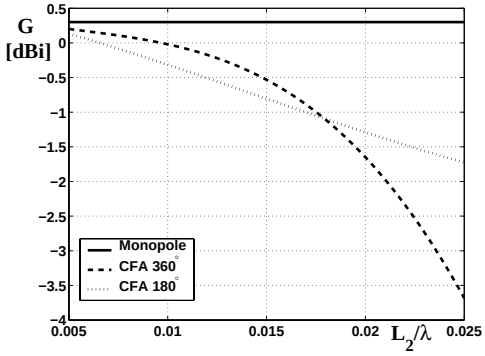


Fig. 24. CFA gain as a function of disk radius $L_2/\lambda$ for a monopole 1 height of $H_1 = 20$ m, at the frequency f = 1 MHz and over average ground.

height of $H_1 = 10$ m and 20 m, over average ground and with tuning coils of merit factor $Q_L = 200$. A reference monopole of the same height has also been calculated.

Antenna gain is shown in Figs. 23 and 24 as a function of disk radius $L_2/\lambda$, where the disk deleterious effect can be clearly appreciated.

Antenna bandwidth is shown in Figs. 25 and 26 as a function of disk radius $L_2/\lambda$, where the disk deleterious effect can also be appreciated.

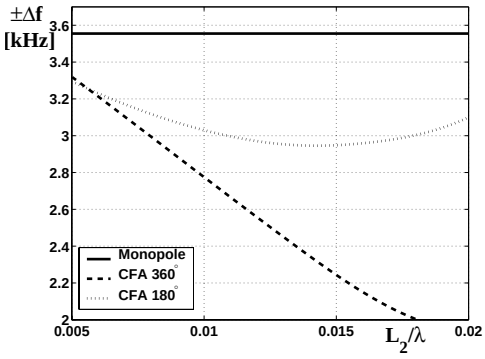


Fig. 25. CFA bandwidth for VSWR = 2 as a function of disk radius $L_2/\lambda$ for a monopole 1 height of $H_1 = 10$ m, at the center frequency f = 1 MHz and over average ground.

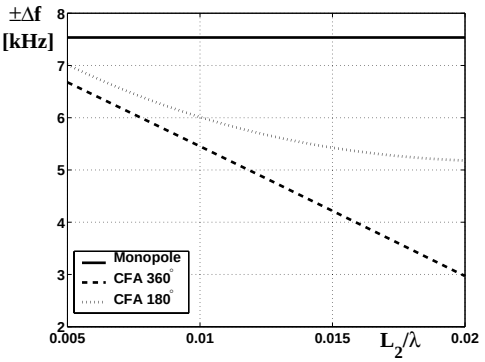


Fig. 26. CFA bandwidth for VSWR = 2 as a function of disk radius $L_2/\lambda$ for a monopole 1 height of $H_1 = 20$ m, at the center frequency f = 1 MHz and over average ground.

### *I. Top-Load Effect*

The CFA antenna performance has been analyzed as a function of the monopole 1 top-load length, $L_1$, with $n = 8$ branches and a constant monopole 1 height of $H_1 = 10$ m over average ground and with tuning coils of merit factor $Q_L = 200$. A reference monopole of the same height and top-load has also been calculated.

In Fig. 27, it can be appreciated an increase in gain as the top-load length $L_1$ is increased for the short monopole and CFA operating in both windows. At the same time, the deleterious effect of the disk is clearly appreciated, because for a larger top-load the monopole and CFA gains are practically the same.

In Fig. 28, the antenna bandwidth is shown, where a better bandwidth for the short monopole can be appreciated in all cases.

It seems this technique of top-load increase was adopted after the previous CFA antenna models. The top-load increase was obtained by means of a conical top-load installed to any CFA, as shown in Fig. 4, in order to improve the input impedance, bandwidth and gain, impossible to be achieved by a short barrel alone used as a vertical monopole. The effect of the top-load cone height $\Delta H_1$ (see Fig. 4) is to increase the antenna effective height, so a similar effect could be achieved increasing the monopole 1 height from $H_1$ to $H_1 + \Delta H_1$ and maintaining the same top-load length $L_1$.

This is a clear demonstration that a very short antenna has always a very sharp frequency behavior and for the CFA antenna this statement is also valid, because it obeys the same antenna theory with no exceptions.

## VIII. Measurements

Far field calculations have been carried out for existing CFA antennas, where measurements are available. Papers of measurements have been evaluated and comparisons with theoretical calculations have been performed.

Nile Delta Tanta (Egypt) CFA antenna operates at 1161 kHz. Field strength data have been released and are shown in [13].

This antenna model has been calculated over a flat ground plane with the same available dimensions, in order to compare with the released field strength data.

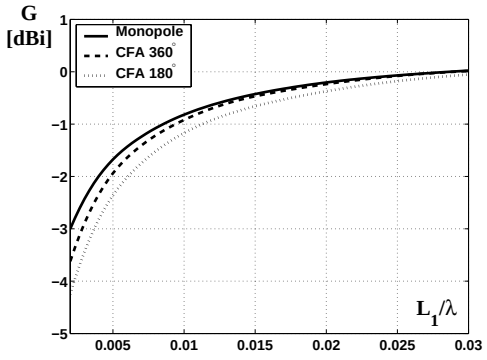


Fig. 27. CFA gain as a function of top-load length $L_1/\lambda$ for a monopole 1 height of $H_1 = 10$ m and a disk radius $L_2 = 2.5$ m, at the center frequency f = 1 MHz and over average ground.

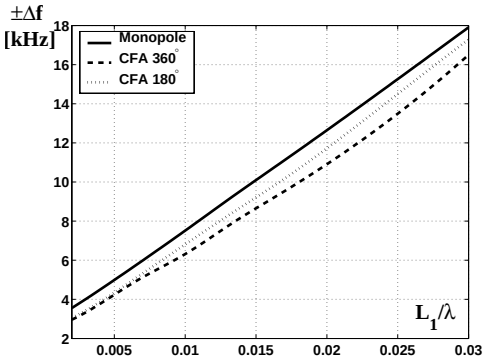


Fig. 28. CFA bandwidth for VSWR $= 2$ as a function of top-load length $L_1/\lambda$ for a monopole 1 height of $H_1 = 10$ m and a disk radius $L_2 = 2.5$ m, at the center frequency f = 1 MHz and over average ground.

Fig. 29 shows the measured values compared to a theoretical short monopole, placed over a perfectly conducting artificial ground plane, and a CFA model over wet ground. Good agreement can be seen and the Tanta CFA has a field strength according to a short antenna placed over a good artificial ground plane.

It is important to know that this antenna was installed over a building with a metallic ground plane laid down in the roof. Metallic straps along the building walls have been installed, connecting the roof ground plane to the actual ground plane at the soil level. This complex ground plane has the effect of increasing the antenna height H and, of course, it increases the antenna efficiency and gain, converting this antenna in a kind of skirted monopole [35], as Fig. 30 shows.

However, measured field strength values are not spectacular and they are within the expected values for this kind of short antenna.

Another example where a CFA antenna was used is the San Remo experiment for a frequency of 1188 kHz. This experimental system was made up by *Rai Way* under the direction of Dr. Alberto Fassio, in order to evaluate its performance. Measurements have been made by RAI engineers and technicians under the direction of Luciano Pautasso. They have used well calibrated field strength instrumentation.

In Fig. 31, RAI field strength measurements are compared by means of a similar theoretical CFA model installed over a

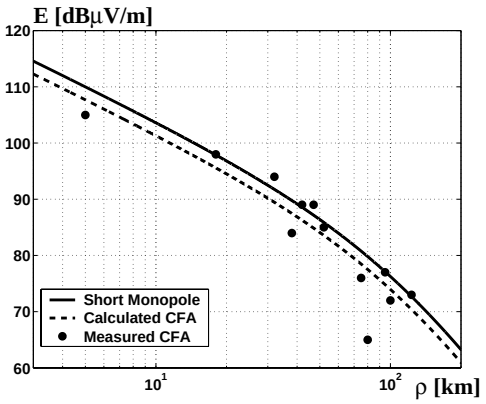


Fig. 29. Measured Tanta CFA field strength as a function of distance $\rho$ compared to a theoretical short monopole and a calculated CFA, on a ground plane of $\sigma = 0.05$ S/m and $\epsilon_r = 20$ for an input power of 30 kW (Tanta CFA was installed on a building roof).

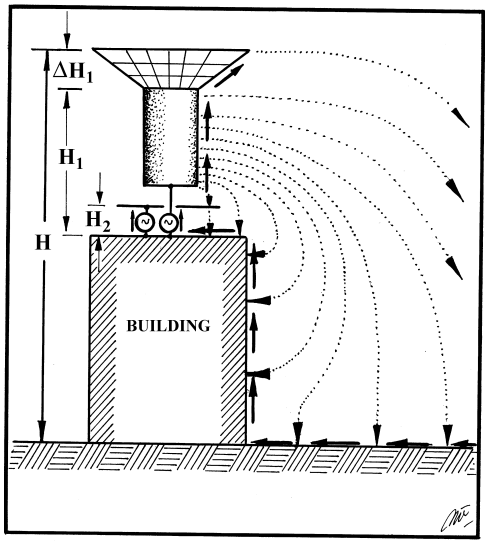


Fig. 30. CFA antenna on a building roof.

flat artificial ground plane and average ground.

San Remo CFA antenna was installed on a transmitting building roof too and a metallic artificial ground plane was laid down over the roof. Building location is close to the Mediterranean sea side, so some measured points are along the sea coast and some others are located inland with different ground constants.

Fig. 31 shows a lower field strength than the theoretical calculations. In some cases, the measured field strength is close to the average ground theoretical curve, but the actual link was performed over sea water.

Due to low measured field strength values, the top-load of this antenna was increased by means of sixteen aluminum tubes, but no increase in field strength was observed due to a very small top-load increase. At the present time, this antenna is not operating because it has been dismantled.

In Brazil, two CFA experimental antennas have been installed in order to determine their performances. One CFA was installed in Sao Paulo by Sylvio Damiani, intended to be used at a frequency of 560 kHz. Personal information

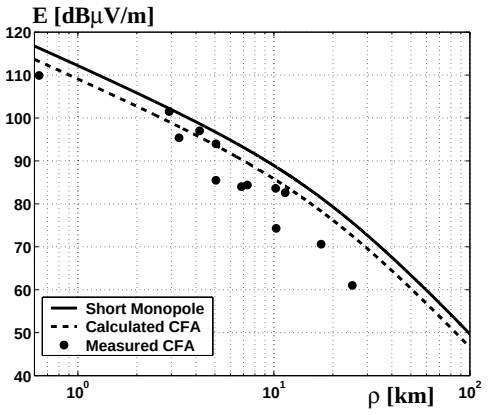


Fig. 31. Measured San Remo CFA field strength as a function of distance $\rho$ compared to a theoretical short monopole and a calculated CFA, on a ground plane of $\sigma = 0.01\ \mathrm{S/m}$ and $\epsilon_\mathrm{r} = 10$ for an input power of 2 kW (San Remo CFA was installed on a building roof).

from Mr. Otavio Emmanuel Lima is that this antenna was never operating better than -10 dB compared to a quarter-wave monopole. No more experiments with this antenna were performed after Sylvio passed away.

Another CFA experimental antenna was installed in Goiania by Mr. Lima for a frequency of 1230 kHz. This antenna was installed on a small building roof 4 m in height and a 12 by 12 m metallic ground plane was laid down over the roof. The antenna monopole 1 was $6.5$ m in height and the metallic disk was 4 m in diameter. Mr. Lima was making a lot of tests on it during long time. Nevertheless, the better field strengths achieved were always 6 dB below, compared to a quarter-wave monopole.

Finally, it was pointed out that a CFA gain improvement is obtained installing it on a building roof. In the case of very low power installations, as the case of the short time CFA experiment performed in Sidney, Australia, (personal communication), an intended 1 kW operation was mandatory decreased by the authority to 200 W, because of neighbor complaints, due to a lot of interferences and disturbances caused to different systems in a crowded area by the radiated AM signal.

## IX. Conclusion

CFA antennas have been exhaustively analyzed. From this analysis, it is pointed out the following:

- A CFA antenna transmission line model has been proposed and its equivalent network has been obtained. At the same time, this model has been validated by means of Moment Method simulations and some available experimental data.
- From this approach, it can be seen three antenna working possibilities according to the sign of the mutual conductance $\mathrm{G}_{12}$.
- Two operating windows, for values of $\phi_2$ near $180°$ or $360°$, and some specific values of K permit having a positive input power in each port.
- Antenna tuning has been obtained connecting the appropriated coils including their merit factors.
- Antenna operation for each $\phi_2$-window has been compared to a reference monopole of the same height and on the same ground plane and top-loading conditions.
- It can be concluded that the disk presence has always a deleterious effect, decreasing the antenna performance.
- The CFA performance is always a little worst than the reference monopole in gain and bandwidth. The antenna performance increases as either the antenna height or top-loading is increased, in the same way as for any standard short monopole. Also, a simple monopole has a similar or better performance with an easier tuning system.
- CFA antenna has the same radiation pattern and near field distribution as any short monopole, then no Poynting Vector Synthesis (PVS) can be seen close to the CFA antenna.
- A CFA gain improvement is obtained installing it on a building roof, in the same manner as for a standard monopole, as it was pointed out since long time in different parts of the frequency spectrum [35].
- It must be pointed out that moderated or high power operations with short antennas does not mean they can be installed in any place, but in conventionally isolated areas as good engineering practice indicate for standard LF and MF AM stations. Of course, this installation place is matter of the Government Administration, due not only to interference but to non ionized radiation levels too.

## Appendix A
## Disk Loss Resistance

CFA disk surface current density on each face is given by

$$\mathrm{J_s} = \frac{1}{2}\,\frac{\mathrm{I}(\rho)}{2\,\pi\,\rho} \tag{54}$$

Where $\mathrm{I}(\rho)$ is given by (46).

The power dissipated in both disk faces, due to the finite metallic disk conductivity, $\sigma_\mathrm{c}$, can be determined by

$$\mathrm{W_d} = 2\int_{\mathrm{r_h}}^{\mathrm{L_2}} |\mathrm{J_s}|^2 \sqrt{\frac{\omega\,\mu_0}{2\,\sigma_\mathrm{c}}}\ 2\,\pi\,\rho\,\mathrm{d}\rho \tag{55}$$

This integral can be carried out to give

$$\mathrm{W_d} = \frac{1}{4\pi}\sqrt{\frac{\omega\,\mu_0}{2\,\sigma_\mathrm{c}}}\,\frac{|\mathrm{I_2}|^2}{(\mathrm{L_2}-\mathrm{r_h})^2}$$
$$\left[\mathrm{L_2^2}\,\ln\left(\frac{\mathrm{L_2}}{\mathrm{r_h}}\right) - 2\,\mathrm{L_2}\,(\mathrm{L_2}-\mathrm{r_h}) + \frac{\mathrm{L_2^2}-\mathrm{r_h^2}}{2}\right] \tag{56}$$

Then, the disk loss resistance, summing up the losses of the vertical feed conductor of height $\mathrm{H_2}$, will be

$$\mathrm{R_{c2}} = \frac{\mathrm{W_d}}{|\mathrm{I_2}|^2} + \frac{\mathrm{H_2}}{\mathrm{a_2}}\sqrt{\frac{\mathrm{f}\,\mu_0}{4\,\pi\,\sigma_\mathrm{c}}} \tag{57}$$

## Appendix B
## Operating Windows

The CFA input power ratio, $\mathrm{K_w}$, is defined as

$$\mathrm{K_w} = \frac{\mathrm{W_2}}{\mathrm{W_1}} \tag{58}$$

Then

$$\mathrm{K_w} = \frac{\mathrm{K^2\,G_{22} + K\,G_{12}\,\cos\phi_2 + K\,B_{12}\,\sin\phi_2}}{\mathrm{G_{11} + K\,G_{12}\,\cos\phi_2 - K\,B_{12}\,\sin\phi_2}} \tag{59}$$

For a given input power ratio $\mathrm{K_w}$, the voltage phase difference $\phi_2$ can be written as a function of K, that is

$$\phi_2(\mathrm{K}) = \pm\arccos\left[\frac{\mathrm{K_w\,G_{11} - K^2\,G_{22}}}{\mathrm{K}\sqrt{(1-\mathrm{K_w})^2\,\mathrm{G_{12}^2} + (1+\mathrm{K_w})^2\,\mathrm{B_{12}^2}}}\right] + \\ + \arctan\left[\frac{(1+\mathrm{K_w})\,\mathrm{B_{12}}}{(1-\mathrm{K_w})\,\mathrm{G_{12}}}\right] \pm \mathrm{m}\,\pi \qquad \mathrm{m} = 0,\ 1,\ 2,\ \ldots \tag{60}$$

The chosen K must verify the following inequality:

$$\left|\frac{\mathrm{K_w\,G_{11} - K^2\,G_{22}}}{\mathrm{K}\sqrt{(1-\mathrm{K_w})^2\,\mathrm{G_{12}^2} + (1+\mathrm{K_w})^2\,\mathrm{B_{12}^2}}}\right| \leq 1 \tag{61}$$

Once a K has been chosen, the $\phi_2(\mathrm{K})$ are calculated and mapped into the $[0, 2\pi)$ interval, where they cover a neighborhood of $\pi$, called the $180°$-window, and neighborhoods of $0$ and $2\pi$, called the $360°$-window (or $0°$-window).

In the case of equal input powers ($\mathrm{K_w} = 1$), it follows that

$$\phi_2(\mathrm{K}) = \pm\arcsin\left[\frac{\mathrm{G_{11} - K^2\,G_{22}}}{2\,\mathrm{K\,B_{12}}}\right] \pm \mathrm{m}\,\pi \qquad \mathrm{m} = 0,\ 1,\ 2,\ \ldots \tag{62}$$

and

$$\left|\frac{\mathrm{G_{11} - K^2\,G_{22}}}{2\,\mathrm{K\,B_{12}}}\right| \leq 1 \tag{63}$$

Thus, for a given total input power $\mathrm{W_{in}}$ and power ratio $\mathrm{K_w}$, the values of $\phi_2$ and K can be obtained from (60) and (61), then the port 1 input voltage will be

$$\mathrm{V_1} = \sqrt{\frac{\mathrm{W_{in}}}{\mathrm{G_{11} + 2\,K\,G_{12}\,\cos\phi_2 + K^2\,G_{22}}}} \tag{64}$$

## Appendix C
## Glossary of Symbols

| | |
|---|---|
| $\mathrm{a_i}$ | i-th monopole wire radius [m]. |
| $\beta$ | Phase constant or wave number ($\beta = 2\pi/\lambda$) [rad/m]. |
| $\mathrm{B_{12}}$ | CFA mutual susceptance [S]. |
| $\mathrm{B_{ii}}$ | i-th monopole self-susceptance [S]. |
| $\mathrm{C_2}$ | Disk capacitance [F]. |
| D | CFA directivity. |
| $\eta$ | CFA efficiency. |
| $\mathrm{E_\theta}$ | Electric field $\theta$-component [V/m]. |
| $\epsilon_\mathrm{r}$ | Soil relative permittivity. |
| G | CFA gain. |
| $\mathrm{G_{12}}$ | CFA mutual conductance [S]. |
| $\mathrm{G_{ii}}$ | i-th monopole self-conductance [S]. |
| $\mathrm{H_e}$ | CFA effective height [m]. |
| $\mathrm{H_{ei}}$ | i-th monopole effective height [m]. |
| $\mathrm{H_i}$ | i-th monopole height [m]. |
| $\mathrm{H_\phi}$ | Magnetic field $\phi$-component [A/m]. |
| i | $= 1,\ 2.$ |
| $\mathrm{I_i}$ | i-th monopole effective input current [A]. |
| $\mathrm{I}(\rho)$ | Disk current distribution [A]. |
| j | $\sqrt{-1}$ imaginary unit. |
| $\mathrm{J_s}$ | Disk surface current density [A/m]. |
| K | Input voltage amplitude ratio. |
| $\mathrm{K_w}$ | Input power ratio. |
| $\mathrm{L_1}$ | Monopole 1 top-load length [m]. |
| $\mathrm{L_2}$ | Disk radius (monopole 2 top-load length) [m]. |
| n | Monopole 1 top-load branches. |
| $\phi_2$ | Input voltage phase difference. |
| $\mathrm{Q_{Li}}$ | i-th monopole coil merit factor. |
| $\rho$ | Radial distance from the antenna base [m]. |
| $\mathrm{r_h}$ | Disk hole radius [m]. |
| $\mathrm{R_0}$ | Artificial ground plane radius [m]. |
| $\mathrm{R_{12}}$ | CFA mutual resistance [$\Omega$]. |
| $\mathrm{R_i}$ | i-th monopole input resistance [$\Omega$]. |
| $\mathrm{R_{ci}}$ | i-th monopole conductor resistance [$\Omega$]. |
| $\mathrm{R_g}$ | Artificial ground plane resistance [$\Omega$]. |
| $\mathrm{R_{gpi}}$ | i-th monopole ground plane loss resistance [$\Omega$]. |
| $\mathrm{R_{ii}}$ | i-th monopole self-resistance [$\Omega$]. |
| $\mathrm{R_{cLi}}$ | i-th monopole conductor resistance per unit length [$\Omega/\mathrm{m}$]. |
| $\mathrm{R_{Li}}$ | i-th monopole tuning coil resistance [$\Omega$]. |
| $\mathrm{R_{rad}}$ | CFA radiation resistance [$\Omega$]. |
| $\mathrm{R_{radi}}$ | i-th monopole radiation resistance [$\Omega$]. |
| $\mathrm{R_s}$ | Soil resistance [$\Omega$]. |
| $\sigma$ | Soil conductivity [S/m]. |
| $\sigma_\mathrm{c}$ | Wire conductivity [S/m]. |
| $\sigma_\mathrm{m}$ | Artificial ground plane (metallic layer) conductivity [S/m]. |
| $\mathrm{V_i}$ | i-th monopole effective input voltage [V]. |
| $\mathrm{W_d}$ | Power dissipated in the disk [W]. |
| $\mathrm{W_i}$ | i-th monopole input power [W]. |
| $\mathrm{W_{in}}$ | CFA input power [W]. |
| $\mathrm{W_{rad}}$ | CFA radiated power [W]. |
| $\mathrm{X_{12}}$ | CFA mutual reactance [$\Omega$]. |
| $\mathrm{X_i}$ | i-th monopole input reactance [$\Omega$]. |
| $\mathrm{X_{ii}}$ | i-th monopole self-reactance [$\Omega$]. |
| $\mathrm{X_{ti}}$ | i-th monopole top-reactance [$\Omega$]. |
| $\mathrm{X_{Li}}$ | i-th monopole tuning coil reactance [$\Omega$]. |
| $\mathrm{Y_{12}}$ | CFA mutual admittance [S]. |
| $\mathrm{Y_{ii}}$ | i-th monopole self-admittance [S]. |
| $\mathrm{Z_0}$ | Near field wave impedance [$\Omega$]. |
| $\mathrm{Z_{00}}$ | Free space intrinsic impedance ($377\ \Omega$). |
| $\mathrm{Z_{0mi}}$ | Equivalent transmission line average characteristic impedance of the i-th monopole [$\Omega$]. |
| $\mathrm{Z_{12}}$ | CFA mutual impedance [$\Omega$]. |
| $\mathrm{Z_i}$ | i-th monopole input impedance [$\Omega$]. |
| $\mathrm{Z_{ii}}$ | i-th monopole self-impedance [$\Omega$]. |
| $\mathrm{Z_g}$ | Artificial ground plane impedance [$\Omega$]. |
| $\mathrm{Z_s}$ | Soil impedance [$\Omega$]. |

## References

[1] V. Trainotti and L. A. Dorado, *Short Low and Medium Frequency Antenna Performance*, 54th Annual IEEE Broadcast Technology Society Symposium Proceeding, October 2004, Reprinted in QEX May-June 2005.

[2] A. Djordjevic, *A Review of the Crossed-Field Antenna*, Private Communication, October 1999.

[3] J. S. Belrose, *The Crossed Field Antenna Analyzed by Simulation and Experiment*, A. P. 2000 Symposium, Davos, Switzerland, April 2000.

[4] J. S. Belrose, *Characteristics of The CFA Obtained by Numerical and Experimental Modeling*, CFA Panel Presentation, 50th. Annual Broadcast Technology Symposium, Vienna, VA, 27-29, September 2000.

[5] J. S. Belrose, *Radiation Characteristics of an Electrically Small MF Broadcast Antenna - By Simulation*, Eleventh International Conference on Antennas and Propagation (ICAP 2001). Manchester, UK, 17-20, April 2001.

[6] V. Trainotti, *Short Medium Frequency AM Antennas*, IEEE Trans. on Broadcasting, vol. 47, no. 3, pp. 263-284, Sept. 2001.

[7] J. S. Belrose, *A CFA on the Roof of a Building*, Private Communication, March 2001.

[8] IEEE-BTS, *CFA Forum*, 50th Annual IEEE Broadcast Symposium, Vienna, VA, 27-29, Sept. 2000.

[9] J. K. Breakall, M. W. Jacobs, A. E. Resnik, G.Y. Eastman, M.D. Machalek, and T. F. King, *A Novel Short AM Monopole Antenna with Low Loss Matching System*, IEEE BTS 52nd, Annual Broadcast Symposium, Oct. 10-11, 2002. Omni Shoreham Hotel, Washington, D.C.

[10] J. K. Breakall, M. W. Jacobs, T. F. King and A. E. Resnik, *Testing and Results of a New Efficient Low-Profile AM Medium Frequency Antenna System*, NAB 2003 Broadcast Engineering Conference Proceedings, pp. 235-243, April 2003.

[11] F. M. Kabbary, M. C. Hately and B. G. Stewart, *Maxwell's Equations and the Crossed Field Antenna*, Electr. World & W. W. 95, pp. 216-218, 1989.

[12] F. M. Kabbary, M. C. Hately and B. G. Stewart, *CFA Working Assumptions*, Electr. World & W. W. 96, pp. 1094-1099, Dec. 1992.

[13] F. M. Kabbary, M. Khattab and M. C. Hately, *Extremely Small High Power MW Broadcasting Antennas*, IEEE International Broadcasting Conference (IBC), Amsterdam, 10-12th Sep. 1997.

[14] F. M. Kabbary, M. Khattab, B. G. Stewart, M. C. Hately and A. Fayoumi, *Four Egyptian MW Broadcast Crossed-Field Antennas*, Proceedings of the NAB Conference, Las Vegas, NV, pp. 235-241, April 1999.

[15] W. C. Alexander, *Is this AM Antenna for real?*, Radio World, March 31, 1999.

[16] M. C. Hately and F. M. Kabbary, *1988, British Patent Application 2,215,524.*

[17] W. C. Johnson, *Transmission Lines and Networks*, Mc. Graw Hill, N. Y., 1950.

[18] J. J. Karakash, *Transmission Lines and Filter Networks*, The Macmillan Company, N. Y., 1950.

[19] W. L. Everitt, *Communication Engineering*, Mc. Graw Hill, N.Y. 1937.

[20] E. Laport, *Radio Antenna Engineering*, Mc. Graw Hill, N. Y., 1952.

[21] J. D. Kraus, *Antennas*, Mc. Graw Hill, N. Y., 1950.

[22] C. A. Balanis, *Antenna Theory Analysis and Design*, John Wiley & Sons, N. Y., 1982, 1997.

[23] W. L. Stutzman and G. A. Thiele, *Antenna Theory and Design*, John Wiley & Sons, N. Y., 1982, 1998.

[24] P. S. Carter, *Circuit Relations in Radiating Systems*, Proc. IRE, vol. 20, no. 6, pp. 1004, June 1932.

[25] L. A. Dorado, EMMCAP$^{(R)}$, *Electromagnetic Modeling Computation and Analysis Program*, http://www.emmcap.com.ar/

[26] E. C. Jordan, *Electromagnetic Waves and Radiating Systems*, Prentice-Hall Inc., N. Y., 1950.

[27] S. A. Schelkunoff and H. T. Friis, *Antenna Theory and Practice*, John Wiley & Sons, N. Y., 1952.

[28] V. Trainotti, *Simplified Calculation of Coverage Area for MF AM Broadcast Station*, IEEE A & P Magazine, pp. 41-44, June 1990.

[29] V. Trainotti, W. G. Fano and L. A. Dorado, *Ingeniería Electromagnética II*, Nueva Librería, Buenos Aires, Argentina, 2005.

[30] J. E. Storer, *The Impedance of an Antenna over a Large Circular Screen*, J. of App. Physics, vol. 22, no. 8, pp. 1058-1066, August 1951.

[31] J. R. Wait and W. J. Surtees, *Impedance of a Top-Loaded Antenna of Arbitrary Length over a Circular Grounded Screen*, J. of App. Physics, vol. 25, no. 5, pp. 553-555, May 1954.

[32] G. H. Brown, R. F. Lewis and J. Epstein, *Ground System as a Factor in Antenna Efficiency*, Proc. IRE, vol. 25, no. 6, pp. 758-787, June 1937.

[33] R. Harrington, *Field Computation by Moment Methods*, Macmillan, N. Y., 1968.

[34] M. C. Hately, F. M. Kabbary and M. Khattab, *An Operational MF Antenna using Poynting Vector Synthesis*, Proceedings of the Seventh International Conference on Antennas and Propagation, Part 2, IEE Conference Publication No. 333, pp. 645-648, April 1991.

[35] Radio Research Laboratory Staff, *Very High Frequency Techniques*, Mc Graw Hill, N.Y. 1947, Vol. 1.

**Valentino Trainotti** was born in Trento, Italy, in 1935. He received the Electronic Engineering Degree from the Universidad Tecnologica Nacional, Buenos Aires, Argentina in 1963.

His post-graduate coursework on antenna measurements and geometric theory of diffraction was completed at California State University in 1981 and Ohio State University in 1985.

He has worked from 1963 to 2003 at CITEFA as the Antenna & Propagation Division Chief Engineer.

His work also includes being on the Engineering Faculty at the University of Buenos Aires as a part-time Full Professor of Electromagnetic Radiation and Radiating Systems for graduated students.

He is an IEEE Senior Member, Member of the IEEE Ad-Com BTS Society, IEEE BT Transactions Associate Editor, IEEE BTS Argentina Chapter Chair, URSI Commission B Argentina Chair, and 1993 IEEE Region 9 Eminent Engineer.

He has worked more than thirty years developing and measuring antenna systems for several applications from LF to SHF.

**Luis A. Dorado** was born in Tucuman, Argentina, in 1976. He received the Electronic Engineering Degree from the Universidad Nacional de Tucuman, Tucuman, Argentina, in 2001, and is currently working toward the Ph.D. degree.

He has developed commercial and academic simulation software related to computational electromagnetics, especially moment method algorithms for computing radiation and scattering from wire structures and antennas.

He is currently working on new numerical and analytical analysis tools and techniques for solving problems in these areas. His research interest include computer simulation of EMC problems and antennas over real ground.